Incorporating free-floating car-sharing into an activity-based dynamic user equilibrium model : a demand-side model

Transportation Research Part B 107 (2018) 102–123

Contents lists available at ScienceDirect

Transportation Research Part B

journal homepage: www.elsevier.com/locate/trb

Incorporating free-floating car-sharing into an activity-based dynamic user equilibrium model: A demand-side model

Qing Li[a,b], Feixiong Liao[b,*], Harry J.P. Timmermans[b], Haijun Huang[c], Jing Zhou[d]

[a] School of Economics and Management, Nanjing University of Information Science and Technology, PR China
[b] Urban Planning Group, Eindhoven University of Technology, The Netherlands
[c] School of Economics and Management, Beihang University, PR China
[d] School of Management and Engineering, Nanjing University, PR China

ARTICLE INFO

Article history:
Received 6 June 2017
Revised 21 November 2017
Accepted 22 November 2017

Keywords:
Activity-travel scheduling
Dynamic user equilibrium
Multi-state supernetwork
Free-floating car-sharing

ABSTRACT

Free-floating car-sharing (FFC) has recently received increasing attention due to the flexibility in mobility services. Existing studies related to FFC mainly focus on the analysis of operational management and user preferences. Efforts to model the dynamic choices of free-floating shared cars (SCs) in individuals' daily multi-modal multi-activity trip chains have still been rare. This study proposes a tolerance-based dynamic user equilibrium model of activity-travel scheduling that formulates free-floating SC as an alternative transport mode for conducting daily activities. The model embeds the choice of SC into daily trip chains by extending the state-of-the-art multi-state supernetwork representation. The dynamic traffic flows and supply-demand interactions of SCs are captured endogenously. Moreover, traveler heterogeneity and different pricing schemes are taken into account. A path-flow swapping method is suggested to solve the tolerance-based dynamic user equilibrium model. Numerical examples of various scenarios demonstrate that fleet size, distribution, and rental-parking price of FFC significantly influence the choice of SC and activity-travel pattern.

1. Introduction

During the past decades, private car (PC) and public transport (PT) have been the two main transport mode alternatives facilitating mobility at the urban scale. Compared with PT, PC usually offers higher travel comfort and allows flexible travel arrangements without the necessity of following particular routes and time schedules. However, as the number of PCs is rapidly increasing, a series of emerging urban problems become significant, including traffic congestion, air pollution, space shortage for parking, etc. As reported in Morgan Stanley (2016), a PC typically sits idle for 23 hours a day, which is a tremendous waste of resources. Along with these mobility problems, there is accumulating evidence, especially for the younger generation, that the importance of owning a car is decreasing (Garikapati et al., 2016). It reflects a more general shift towards a shared economy which can also be observed in other industries. As a promising way to ease aforementioned urban issues, car-sharing has recently attracted increasing attention in both practice and academia. As argued by Kortum and Machemehl (2012), in upcoming years urban and transportation planning organizations will be faced with a high need to estimate modal split for car-sharing as it becomes a more pervasive alternative.

* Corresponding author.
E-mail address: f.liao@tue.nl (F. Liao).

https://doi.org/10.1016/j.trb.2017.11.011
0191-2615/

Currently, four common types of car-sharing programs have been developed: traditional round-trip based car-sharing (RTC), station-based one-way car-sharing (SOC), peer-to-peer car-sharing (PPC) and free-floating car-sharing (FFC). While PPC is a customer-to-customer mobility initiative enabling the shared usage of PC, the others are offered by commercial organizations. As for RTC, it is easy for the suppliers to manage inventories while it may cause inconvenience to the users since they have to pay the trips to return the cars. By contrast, SOC is better suited for users but may result in the problem of creating unbalanced vehicle supply and demand across different service stations due to the uneven nature of travel demand. At a more flexible level, shared cars (SCs) of FFC can be picked up and left behind at any regular parking locations within large designated areas. Given the flexibility, FFC is expected to be the main car-sharing program in the near future, especially with the advent of autonomous cars.

However, FFC potentially brings more complexity in the supply and demand of SCs than SOC. Existing studies of FFC mainly focus on the analysis of user preferences and operational management given particular demand patterns (Weikl and Bogenberger, 2015). Activity-based modeling is a promising way to tackle travelers' daily multi-modal multi-activity trip chains. It has been applied to addressing different types of mobility services (Childress et al., 2015; Chow and Djavadian, 2015; Ciari et al., 2016; Nourinejad et al., 2016; Djavadian and Chow, 2017). Motivated by the need to address the flexibility and complexity of FFC and the desire to capture the influence of the free-floating SCs on urban mobility, this study focuses on modeling the supply-demand interactions of free-floating SCs in multi-modal transportation networks. In particular, allowing using SCs for specific trips of full-day trip chains, this study is carried out in the activity-based modeling paradigm that conceptualizes travel as derived demand for conducting activities.

The aim of this study is, therefore, to incorporate FFC in a tolerance-based activity-based dynamic user equilibrium (DUE) model through multi-state supernetwork representation. The model supports the analysis of FFC patronage and assessments of operational strategies with the consideration of travelers' bounded rationality. To that end, the remainder of this study is organized as follows. The next section reports the results of a literature review on the modeling of supply and demand of SCs, based on which the contributions of this study are articulated. Section 3 discusses the multi-state supernetwork representation of trip chains and presents the basic considerations. The dynamic process of using free-floating SCs is illustrated through an example of conducting one activity. Section 4 discusses the disutilities of activity-travel links and patterns in the multi-state supernetworks. Next, the activity-based DUE model in the discrete-time domain and its equivalent variational inequality problem are formulated. A path-flow swapping algorithm is suggested to find the tolerance-based DUE states. Section 6 illustrates the proposed model with numerical examples showing that fleet size, distribution, and rental-parking price influence both the choice of SC and the activity-travel pattern (ATP). Finally, the study is completed with conclusions and a plan for future work.

1.2. Abbreviations

The following primary abbreviations are used in this study.

Abbreviation	*Full name*	*Abbreviation*	*Full name*
PT	Public transport	PC	Private car
PVN	Private vehicle network	SC	Shared car
PTN	Public transport network	FFC	Free-floating car-sharing
IVT	In-vehicle time	RTC	Round-trip based car-sharing
ATP	Activity-travel pattern	SOC	Station-based one-way car-sharing
DUE	Dynamic user equilibrium	PPC	Peer-to-peer car-sharing

2. Literature review

The recent literature exhibits an abundant number of studies on the acceptance, effects, and efficiency of car-sharing programs. Kopp et al. (2015) compared travel behavior of members and non-members of FFC based on a GPS tracking application and found that members of FFC are more intermodal and multimodal. To investigate the factors influencing the demand of SCs, Schmöller et al. (2015) identified the factors influencing the choice of FFC and differentiated between short-term and long-term impacts. Bansal et al. (2016) studied public opinions on shared autonomous vehicles and found that the adoption rate is mainly influenced by the convenience of parking and vehicle ownership rate of the city. Zoepf et al. (2016) focused on how users value price, distance, schedule and vehicle type, and found that vehicle availability at their desired time and location had the most utility impact and might shift users' schedules. Based on discrete choice modeling, De and Di (2015) investigated the effects of a SOC program on users' mode choice and concluded that travel cost, availability and the type of trip significantly influence the probability of choosing SC. Kim et al. (2017) developed a regret-based hybrid model and concluded that uncertainty and socio-demography influence substantially car-sharing decisions.

Another stream of literature has explored mathematical programming approaches to support optimal management. As for SOC, models have been proposed to investigate the fleet size, distribution, parking reservation, and vehicle relocation (Cepolina and Farina, 2012; Nourinejad and Roorda, 2015; Hu and Liu, 2016; Kaspi et al., 2016; Boyacı et al., 2017). A few studies have addressed the problem of fleet size management and relocation for FFC. For instance, Kortum and Machemehl (2012) modeled the optimal allocation for multiple demand periods within one day. In their study, when the

Table 1
Previous studies on supply and demand of SC.

Objectives	References	Activity-based	Multi- modal	User equilibrium	Car-sharing System
Optimal fleet size	Cepolina and Farina (2012)	Y	Y	N	SOC
	Barrios and Godier (2014)	N	N	N	SOC/FFC
	Nourinejad and Roorda (2015)	Y	N	N	RTC/SOC
	Hu and Liu (2016)	N	N	N	SOC
Relocation strategies	Clemente et al. (2013)	N	N	N	SOC
	Jorge et al. (2015)	N	N	N	SOC
	Weikl and Bogenberger (2015)	N	N	N	FFC
	Boyacı et al. (2017)	N	N	N	SOC
Reservation policies	Kaspi et al. (2014)	N	Y	N	SOC
	Kaspi et al. (2016)	N	Y	N	SOC
Demand analysis	Ciari et al. (2013)	Y	Y	Y[a]	RTC
	Ciari et al. (2016)	Y	Y	Y[a]	FFC
	Balac et al. (2017)	Y	Y	Y[a]	FFC
	Heilig et al. (2017)	Y	Y	N	RTC/FFC
Demand analysis	*Current study*	Y	Y	Y	FFC

(Y and N: with and without the referred element respectively; [a] microsimulation-based framework)

demand is unsatisfied by the available SCs at the current period, travelers are assumed to wait until cars became available. However, there is no threshold for waiting time, which means if no SC is available, travelers will keep waiting all the time. Weikl and Bogenberger (2015) presented a practice-ready relocation model with both conventional vehicles and electric vehicles, detailing the relocation zone into macroscopic and microscopic zones to investigate inter-zonal and intra-zonal relocation. Jorge et al. (2015) defined the derivation of the supply and demand of SCs at each operational area and period but independent of the attributes of the activities. Also, several comprehensive literature overviews on car-sharing programs have been provided, e.g., on demand forecasting and relocation operation (Jorge and Correia, 2013) and the research gaps of existing relocation models for FFC (Weikl and Bogenberger, 2015). Overall, these analyses mainly focused on car-sharing operational management at the system level, rather than on the demand side confronting the multi-modal transportation systems.

To model the demand side, Ciari et al. (2013) estimated travel demand for RTC based on an activity-based a microsimulation system (MATSim). However, the study assumed that the number of available SCs at a station was unlimited. To address the limitation, Ciari et al. (2016) improved the simulation model for FFC system, but the model could still not capture the influence of supply on mobility patterns. Balac et al. (2017) further investigated the supply-demand interactions in the context of FFC. Similarly, Heilig et al. (2017) adopted the microsimulation framework of mobiTopp for multi-day operations to capture the dynamic interactions.

Table 1 summarizes the recent studies on modeling the supply and demand of car-sharing systems. As shown, studies focusing on the supply side ignore the facts that travel is triggered by activity participation and multi-modal trip chaining is an inevitable component. These facts have been well recognized in microsimulation-based studies for demand analysis. Moreover, the concept of simulated user equilibrium has been applied in MATSim via an iterative probabilistic process. Microsimulation-based studies are dedicated to large-scale, high-resolution analyses. However, they need to couple exogenous modules of disaggregate activity-travel scheduling and aggregate traffic assignment that potentially cause inconsistent ATPs in space-time. On the other hand, activity-based dynamic user equilibrium (DUE) through supernetworks is promising to remedy this limitation and derives insightful effects of policy scenarios (e.g. Li et al., 2010; Ramadurai and Ukkusuri, 2010; Fu and Lam, 2014; Liu et al., 2015; Li et al., 2016). A review of this line of model development shows that hitherto none has incorporated SC in an activity-based DUE model.

With a focus on the demand side, this study addresses activity-based DUE after incorporating FFC given specific supply scenarios at the beginning of a typical day. With FFC, the vehicles are supposed to be rebalanced by the travelers. Given sufficient fleet size, reservation deems unnecessary, and travelers with smartphone-based applications exactly know when SCs will be rebalanced within a short time frame. Thus, we leave the investigation of reservation and relocation strategies implemented either by service providers or self-driving SCs (Lamotte et al., 2017) in a sequel of studies focusing on the supply side. The main contributions of the current research are positioned in the realm of network-based analysis, including the following features (from this place onwards, SC refers to FFC unless otherwise noted):

(1) incorporating FFC in an activity-based DUE model, that captures multi-modal and multi-activity trip chaining and modal substitution effects at different stages;
(2) modeling the evolution of SCs in the temporal and spatial dimension, including the traffic flows in the multi-modal transport network and the supply-demand interactions at the SC parking stations;
(3) and allowing the analysis of choice behavior facing different scenarios of FFC services concerning time-dependent pricing schemes, fleet size, and distribution.

3. Basic considerations

3.1. Assumptions

The following assumptions are made to facilitate the presentation of the essential ideas.

A1 The study time horizon [0, T] is discretized into a finite set of equal time intervals, i.e., $\{1, 2, \ldots, \bar{T}\}$. Let Δ be the duration of each time interval such that $\Delta \cdot \bar{T} = T$.

A2 Three transport modes are considered, i.e., PC, PT, and SC. Only one FFC operator exists in the multi-modal transportation system, given the focus of studying DUE from the demand side.

A3 Traveler heterogeneity is considered based on the membership of FFC and different types of time-money valuations.

A4 PT vehicles use separated tracks and follow a scheduled timetable. Stochastic disturbances on the travel times are not considered.

A5 When the demand of SCs exceeds the supply at a location, travelers will either wait until this demand is satisfied or switch to other modes. Travelers are assumed to follow the FIFO (first-in-first-out) principle when waiting for SC. That is to say, travelers who arrive earlier at an SC parking location will always be served first. In case the supply of SCs is sufficient, all demands of SCs will be met simultaneously. If there is a deficiency, travelers arriving earlier have the right of using SCs first. When the stock is replenished, those unsatisfied earlier arrivals will be given the right first. This assumption is realistic when Δ is sufficiently small.

A6 Travelers access SCs depending on the availability, while they can egress SCs at any designated locations. The fee paid to the operator depends on the access time and service duration. SCs are allowed to be parked and picked-up in large designated areas.

A7 Travelers choose ATPs of disutilities within a minor tolerance of the least due to bounded rationality (Simon, 1955; Conlisk, 1996; Hensher, 2010).

3.2. Notations

Primary notations used in this study are defined as follows:

t, t', k, ω	time intervals
Δ	length of a time interval
ε	tolerance level
a, a'	travel or activity links
p	an ATP (path) including travel and activity links
m	a traveler class, $m = 1, 2, \ldots$
Q^m	travel demand of class m
L	a set of locations (nodes)
h	a home location (the start and end point of ATPs)
$l, \hat{l}, l', l''$	locations, $l, \hat{l}, l', l'' \in L$
A	a set of links
A^v,A^a	sets of travel and activity links respectively, $A = A^v \cup A^a$
A_c^v, A_t^v, A_s^v	sets of travel links by PC, PT, and SC respectively, $A^v = A_c^v \cup A_t^v \cup A_s^v$
$y(a)$	the physical road of link a which may be shared by PC and SC
$u_a^{ml\hat{l}}(t)$	link arrival flow of class m at l of a during t; note that l and $\hat{l}$ by their appearance of sequence denote the entry and exit nodes of link a ($l \to \hat{l}$) respectively
$r_a^{ml\hat{l}}(t)$	link inflow on a of m during t
$v_a^{ml\hat{l}}(t)$	link outflow on a of m during t
$x_{y(a)}^{l\hat{l}}(t)$	queue on the physical road of a during t
$S_l(t)$	supply of SC at l during t
$D_l(t)$	demand of SC at l during t
$sk_l(t)$	stock of SC at l during t
$sg_l(t)$	shortage of SC, which refers to the unsatisfied demand* at l during t
$\lambda_0^m, \lambda_1^m, \lambda_2^m$	disutility coefficients of waiting time, IVT, and monetary cost
τ_a	fare per interval on a (ticket cost for PT and fuel cost for PC)
$\tau_a^{l,c}(t)$	rental cost per interval for SC rented at l during t
$\tau_a^{l,r}(t)$	parking cost per interval for SC and PC at l during t
ϕ_a	a progression of departure times of PT vehicles on link a
t_a^0	free flow IVT of link $a \in A^v$
$t_a^{ml\hat{l}}(t)$	IVT on travel link a of m when travelers arrive l during t
$t_a^{ml,w}(t)$	potential waiting time on a of m arriving at l t
d_a^{ml}	duration of activity link a of m at l
$disU_a^{ml\hat{l}}(t)$	disutility of a of m during t
$disU_a^{ml\hat{l},r}(t)$	disutility of parking at $\hat{l}$, which is the exit node of link $a \in A_c^v \cup A_s^v$ of m during t
δ_{at}^{hpk}	0–1 indicator variable: $\delta_{at}^{hpk} = 1$ if travelers depart from h via p during k and arrive at the entry node of a during t; otherwise, $\delta_{at}^{hpk} = 0$
$f_{hp}^m(k)$	departure flow on p from h during k of class m
$PU_{hp}^m(k)$	path disutility of m departing from h during k via p

*During t, if the supply can't satisfy the demand, the current demand will be shifted to next interval.

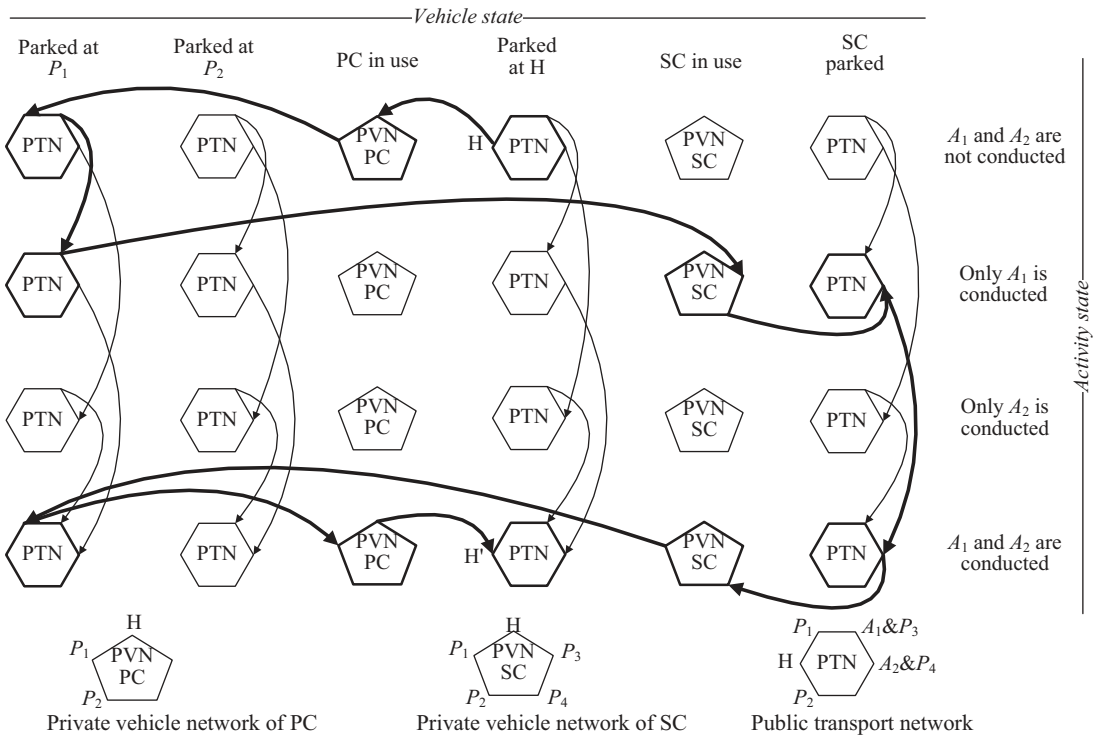

Fig. 1. Example of multi-state supernetwork including SC.

3.3. Incorporating FFC in multi-state supernetworks

Network extensions are instrumental to modeling high dimensional choice problems. Inspired by multi-modal supernetworks (Sheffi, 1985; Nagurney, 2004), Arentze and Timmermans (2004) suggested multi-state supernetworks for representing multi-modal multi-activity trip chains. The essence of multi-state supernetworks is that the activity-travel scheduling process is decomposed into path choice through different states of conducting activities. Liao et al. (2010) further improved the multi-state supernetwork representation to efficiently capture the interdependencies of trip chains. Modeling extensions include park and ride (Liao et al., 2012), joint travel (Liao et al., 2013a), time-dependency (Liao et al., 2013b), uncertainty (Liao et al., 2014), activity-travel assignment (Liu et al., 2015), and alternative choice mechanisms (Li et al., 2016). These extensions make the original framework much more powerful in dealing with activity-travel scheduling problems.

Incorporating FFC into multi-state supernetworks requires a new definition of vehicle state, which initially defines whether the vehicle is in use or parked somewhere. Suppose traveler i is a member of FFC program. When using PC, i has to go to the specific parking location to pick it up first; thus, the supernetwork representation needs to create vehicle states to trace where the car is parked. When using SC, i's actions include picking-up one if it is available, driving to another location either for switching to PT or conducting an activity, and parking SC at the destination. Once it is parked, it is not necessary for i to pick it up again at the same parking location because other travelers may use it. However, if the SC is not available at the pick-up location, i needs to wait until other travelers park SC at that location. If i is unwilling to wait, i may proceed the trip with another transport mode. Thus, in case of using SC, only two vehicle states are needed, i.e., being in use and being parked.

Let $SNK(L, A)$ be a multi-state supernetwork representation of conducting an activity program, where home locations are both the origin to start and the destination to end the ATPs. L denotes a location set in space, and A is a set of links, including travel links (A^v) and activity links (A^a). Travel links represent the movement between two locations involving three different modes: PC (A_c^v), PT (A_t^v) and SC (A_s^v). An example of an ATP through $SNK(L, A)$ incorporating FFC is shown in Fig. 1, which includes activities $A1$ and $A2$ at fixed locations (activity location choice is not shown for simplicity), parking locations $P1$ and $P2$ for both PC and SC, $P3$ and $P4$ only for SC. Pentagons and hexagons denote PVNs (private vehicle networks) and PTNs (public transport networks) respectively. The vertices denote locations, and undirected links are bi-directed links.

In Fig. 1, the path formed by the bold links represents an ATP in which the individual leaves home by PC with parking at $P1$ to conduct activity $A1$, then shifts to SC to conduct $A2$, and finally returns $P1$ by SC to pick up PC, and returns home by PC. For clear representation, only one ATP is illustrated. Other ATPs can be realized by interconnecting PTNs and PVNs of different states. All travel links and transaction links are exhaustively shown. Instead, only those links for parking/picking-up car in the bold path are given. Those links that are not in bold are either travel links inside PVNs/PTNs or transaction

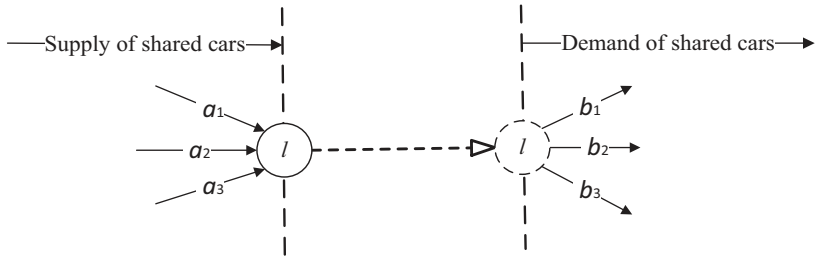

Fig. 2. The supply and demand at a location for car-sharing.

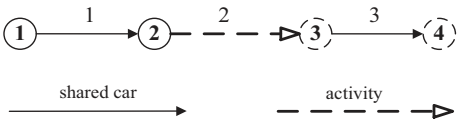

Fig. 3. An example of an activity-travel path.

Table 2
Evolution of traffic flow and supply-demand interaction.

t	$f(t)$	$u_1^{12}(t)$	$v_1^{12}(t)$	$u_2^{23}(t)$	$v_2^{23}(t)$	$u_3^{34}(t)$	$v_3^{34}(t)$
0	0	0	0	0	0	0	0
1	5	5	0	0	0	0	0
2	4	4	5	5	0	0	0
3	4	4	–	–	5	5	0
4	–	–	–	–	–	–	5
5	–	–	8	8	0	0	0
6	–	–	–	–	8	8	0
7	–	–	–	–	–	–	8

t	$sk_1(t)$	$sg_1(t)$	$S_1(t)$	$D_1(t)$	$sk_2(t)$	$sg_2(t)$	$S_2(t)$	$D_2(t)$
0	8	0	0	0	0	0	0	0
1	3	0	8	5	0	0	0	0
2	3	4 **(0)**	3	4	5	0	5	0
3	3	8 **(0)**	3	8	0	0	5	5
4	0	0	8	8	0	0	0	0
5	0	0	0	0	8	0	8	0
6	0	0	0	0	0	0	8	8
7	8	0	8	0	0	0	0	0

(The numbers in the parentheses denote the updated unsatisfied demands at interval 4.)

links in-between PTNs. Fig. 1 only exhibits the spatial representation. If a pattern involves using SC at a location while SC is deficient, i needs to wait. Until SC being rebalanced, the individual proceeds along the pattern. Thus, the state "SC rebalanced" is in the temporal dimension, which is not represented but implicitly addressed in the dynamic process.

3.4. Supply-demand interaction of SCs

Given the characteristics of FFC, the number of SCs at a location at a certain time interval depends on the supply-demand dynamics. Taking a simple network (Fig. 2) for example, during a time interval, the supply of SCs at location l is the sum of the existing stock and the outflows of all SC travel links (e.g., a_1,a_2 and a_3) whose exit nodes are l. The demand of SCs at l is the sum of the existing shortage (unsatisfied demand) if any and the arrival flows of all SC travel links (b_1, b_2 and b_3) whose entry nodes are l. Unsatisfied demand occurs when the demand exceeds the supply, and travelers may have to wait until the supply meets the demand.

To illustrate the dynamic process, Fig. 3 shows a simplified example of the supply-demand interaction on one ATP that starts from location 1 via SC travel link 1 to location 2 to conduct an activity and returns to location 1 via SC travel link 3 after conducting the activity. In Fig. 3, location 1 and 4 represent the same location (origin and destination), and location 2 and 3 are same locations (activity location). Let $f(t)$ be the traffic inflow for path (1–2–3) at a time interval t. According to the notations defined in Section 3.1, the arrival flow and outflow on link 1 are $u_1^{12}(t)$ and $v_1^{12}(t)$ respectively (the notation for class is omitted for simplicity). The stock, shortage, demand, and supply of SCs at location 1 are $sk_1(t), sg_1(t)$, $D_1(t)$, and $S_1(t)$ respectively. The notations apply to other specific locations and links as well. Table 2 gives the evolution of traffic flow

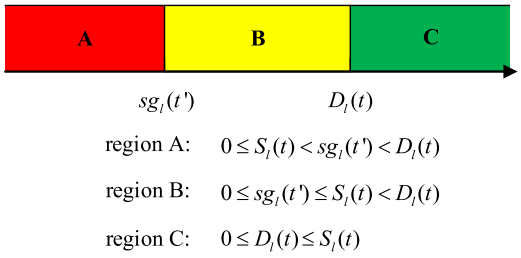

Fig. 4. Relationships among $D_l(t)$, $S_l(t)$ and $sg_l(t')$.

and the stock, shortage, demand and supply of SCs at location 1 (or 4) and 2 (or 3). Time elapse of a link is assumed to be one time interval.

In this example, $f(t)$, $u_1^{12}(t)$ to $\forall t$ and $sk_1(0)$ are given at the start. The supply of SCs at $t=1$ is known as $S_1(1)=8$ and $S_2(1)=0$. The demand of SCs at location 1 at $t=1$ equals to the arrival flow of link 1, i.e. $D_1(1)=u_1^{12}(1)=5$, which is less than $S_1(1)$. Since the traverse time on each link is one interval, all these travelers will exit link 1 at $t=2$ and return to location 1 at $t=4$. Then, we have $u_1^{12}(2)=D_1(2)=4$ and $sg_1(1)=0$, and $S_1(2)$ is updated as 3, which is insufficient to satisfy $D_1(2)$. According to assumption **A5**, these travelers should wait. Thus, the unsatisfied demand is 4 at $t=2$, i.e., $sg_1(2)=4$. With $u_1^{12}(3)=4$, the demand at location 1 is the sum of the new arrival flow and the unsatisfied demand of the last interval, i.e., $D_1(3)=u_1^{12}(3)+sg_1(2)=8$. Since the flow return at location 1 of $u_1^{12}(1)$ at $t=4$ is $v_3^{34}(4)$, supply $S_1(4)$ is the sum of the stock of the last interval and those returned, i.e., $S_1(4)=v_3^{34}(4)+sk_1(3)=8$. As there is no arrival flow to link 1 after interval 3, we have $D_1(4)=u_1^{12}(4)+sg_1(3)=8$, which is met by the supply $S_1(4)$. The unsatisfied demands at and before interval 4 are updated as 0. Thus, travelers of $u_1^{12}(2)$ and $u_1^{12}(3)$ depart together after waiting 2 intervals and 1 interval respectively.

As the example shows, the unsatisfied demand during the last intervals is updated as 0 when the current supply meets the current demand. Thus, the relationship among the current supply, the current demand, and the past unsatisfied demand can be inferred in Fig. 4 with $t' < t$.

The current supply may fall in one of three different regions as follows:

- region A, where the current supply can satisfy neither the current demand nor any of the past unsatisfied demand at the location, no one can pick up SC at l at t;
- region B, where the current supply cannot satisfy the current demand but a past unsatisfied demand, only those past unsatisfied demand can pick up SC at l at t;
- region C, where the current supply exceeds the current demand, all travelers can depart with SC.
- The above supply-demand interactions at the locations are formulated below.

4. Activity-travel path disutility

This section details the formulations of the link and ATP disutilities through the multi-state supernetworks. The disutility of an ATP equals to the summation of the disutilities of the associated activity-travel links. Each supernetwork representation corresponds to one O-D pair and represents the ATP space for travelers who live in the same zone and have the same daily activity program. In an urban system, there are multiple O-D pairs originated from different home zones, which refer to the demand side. On the other hand, facilities of transport and activity locations refer to the supply side that can be accessed by travelers. Given the focus on the demand side, the model framework does not explicitly consider the FFC supply policies, such as reservation policies, relocation strategies, and service areas.

4.1. Disutility of travel links

This subsection formulates the travel link disutilities of three transport modes. Travel-related disutility is derived from waiting time, in-vehicle time (IVT), fare, and parking costs. The access/egress times to/from locations or transport modes are not considered. The time elapse of a travel link consists of waiting time and IVT. Waiting occurs if service time of a transport mode is later than the arrival time. While IVT by PT is assumed to be fixed (**A4**), IVT by PC or SC is determined by the link characteristics and traffic flow conditions at the moment of calculation.

4.1.1. Private car (PC)

When using PC, there is no waiting time and the IVT is dynamically determined by the queue on a link. As assumption **A4** puts, PT vehicles follow separated tracks and do not affect road traffic. As PC and SC share the physical roads, IVT of PC is also influenced by the traffic flow of SC. Thus, the link queue is made of PC and SC, based on which IVT can be written as an extended BPR (Bureau of Public Roads) function. Waiting time and IVT by PC are formulated respectively as

$$t_a^{ml,\mathrm{w}}(t)=0,\ \ a\in A_c^v \tag{1}$$

$$t_a^{ml\hat{l}}(t) = t_a^0 + \eta_a \cdot \left(\frac{x_{y(a)}^{l\hat{l}}(t)}{c_a^{l\hat{l}}} \right)^{\gamma_a}, \ a \in A_c^v \tag{2}$$

where l and $\hat{l}$ are the entry and exit nodes of travel link a by PC respectively. $y(a)$ denotes the physical road of a, which may be shared by PC and SC. t_a^0 and $c_a^{l\hat{l}}$ are the free-flow travel time and road capacity. η_a and γ_a are road-specific parameters resembling those in a BPR function that can be estimated from historical data. $x_{y(a)}^{l\hat{l}}(t)$ is the queue on $y(a)$ contributed by PC and SC. The calculation of $x_{y(a)}^{l\hat{l}}(t)$ will be formulated in Section 5. Hence, travel link disutility by PC is

$$disU_a^{ml\hat{l}}(t) = \lambda_1^m \cdot t_a^{ml\hat{l}}(t) + \lambda_2^m \cdot \tau_a \cdot t_a^{ml\hat{l}}(t), \ a \in A_c^v \tag{3}$$

where $\lambda_1^m (> 0)$ and $\lambda_2^m (> 0)$ are the disutility coefficients of IVT and money expense of class m respectively, and τ_a is the fare per interval on $a \in A_c^v$.

4.1.2. Public transport (PT)

For taking PT, waiting time is the time difference between the arrival time and the next earliest departure time of a PT vehicle. According to **A4**, we obtain the waiting time

$$t_a^{ml,\mathrm{w}}(t) = \min\left\{t' | t' \geq t, \ t' \in \phi_a\right\} - t, \ a \in A_t^v \tag{4}$$

where ϕ_a is a progression of departure times of PT vehicles on link $a \in A_t^v$ and t' is a time instance in φ_a equal to or larger than arrival time t. IVTs of PT links are fixed, i.e., $t_a^{ml\hat{l}}(t) = t_a^0$, $\forall a \in A_t^v$. However, due to the finite capacity of PT vehicles, travelers may experience discomfort due to crowding, which leads to the "feeling" of longer IVT than the actual (Lo et al., 2003). We describe the virtual longer IVT $\tilde{t}_a^{ml\hat{l}}(t)$ by a BPR function as

$$\tilde{t}_a^{ml\hat{l}}(t) = t_a^0 \cdot \left(1 + \eta_a \cdot \left(\frac{\max\left(0, \sum_m r_a^{ml\hat{l}}(t) - \vartheta^m \cdot c_a^{l\hat{l}}\right)}{c_a^{l\hat{l}}} \right)^{\gamma_a} \right), \ a \in A_t^v, \ t, \ t^- \in \phi_a \tag{5}$$

where t_a^0 and $c_a^{l\hat{l}}$ are the actual IVT and capacity of a respectively. $r_a^{ml\hat{l}}(t)$ is the inflow of m on a at t, equaling to $\sum_{\omega=t^-+1}^{t} u_a^{ml\hat{l}}(\omega)$, where $u_a^{ml\hat{l}}(\omega)$ is the arrival flow during interval ω that will depart at t. t^- and t are two consecutive elements in φ_a, satisfying $t^- < t$. ϑ^m is the crowding perception of class m, and if the total in-vehicle flow exceeds $\vartheta^m \cdot c_a^{l\hat{l}}$, travelers will experience discomfort. η_a and γ_a are link-specific parameters to describe the crowding effects. Combining the disutility of waiting, IVT and money expense, the travel disutility of a PT link is

$$disU_a^{ml\hat{l}}(t) = \lambda_0^m \cdot t_a^{ml,\mathrm{w}}(t) + \lambda_1^m \cdot \tilde{t}_a^{ml\hat{l}}\left(t + t_a^{ml,\mathrm{w}}(t)\right) + \lambda_2^m \cdot \tau_a \cdot t_a^0, \ a \in A_t^v \tag{6}$$

where $\lambda_0^m (> 0)$ is the disutility coefficient for waiting time of class m. With waiting, the actual departure time on a is $t + t_a^{ml,\mathrm{w}}(t)$. $\tau_a \cdot t_a^0$ means the fixed price for traversing link a.

4.1.3. Shared car (SC)

As demonstrated in Section 3.3, the stock $sk_l(t)$ or shortage $sg_l(t)$ of SCs at location l is time-dependent and influenced by supply $S_l(t)$ and demand $D_l(t)$. Note that l belongs to a location subset where parking and picking-up SCs is allowed. When $D_l(t) \geq S_l(t)$, as **A5** suggests, travelers wishing to take SC may wait until the updated supply $S_l(t')$ at a later time interval t' satisfies the demand $D_l(t)$. The potential waiting time $t_a^{ml,\mathrm{w}}(t)$ of travelers who arrive l at t is expressed as Eq. (7). $S_l(t)$, $sk_l(t)$, $D_l(t)$ and $sg_l(t)$ at l for travelers arriving at a during t are formulated as Eqs. (8)–(11).

$$t_a^{ml,\mathrm{w}}(t) = \underset{t'}{\operatorname{argmin}}\left\{sg_l(t) \leq S_l\left(t'\right)\right\} - t, \ t' \geq t, \ a \in A_s^v \tag{7}$$

$$D_l(t) = \sum_m \sum_{a, \ \hat{l}} u_a^{ml\hat{l}}(t) + sg_l(t-1), \ a \in A_s^v \tag{8}$$

$$S_l(t) = \sum_m \sum_{a,\hat{l}} v_a^{ml\hat{l}}(t) + sk_l(t-1), \ a \in A_s^v \tag{9}$$

$$sg_l(t) = \begin{cases} D_l(t), & 0 \leq S_l(t) < sg_l(\underline{t}) < D_l(t) \\ D_l(t) - sg_l\left(\tilde{t}\right), & 0 \leq sg_l\left(\tilde{t}\right) \leq S_l(t) < D_l(t) \\ 0, & 0 \leq D_l(t) \leq S_l(t) \end{cases} \tag{10}$$

$$sk_l(t) = \begin{cases} S_l(t), & 0 \le S_l(t) < sg_l(\underline{t}) < D_l(t) \\ S_l(t) - sg_l(\bar{t}), & 0 \le sg_l(\bar{t}) \le S_l(t) < D_l(t) \\ S_l(t) - D_l(t), & 0 \le D_l(t) \le S_l(t) \end{cases} \tag{11}$$

where $u_a^{ml\hat{l}}(t)$ is the arrival flow on link a at entry node l during t, $v_a^{m\hat{l}l}(t)$ is the outflow at exit node l, $\underline{t} = \underset{t'}{\text{argmin}}\{0 < sg_l(t'), t' < t\}$, and $\bar{t} = \underset{t'}{\text{argmax}}\{0 < sg_l(t') \le S_l(t), t' < t\}$. When $0 \le sg_l(\bar{t}) \le S_l(t) < D_l(t)$, $sg_l(t')$ should be updated as Eq. (12); when $D_l(t) \le S_l(t)$, the shortages at location l before interval t should be updated as 0 in Eq. (13).

$$sg_l(t') = \begin{cases} sg_l(t') - sg_l(\bar{t}), & \bar{t} < t' \le t \\ 0, & t' \le \bar{t} \end{cases}, \quad 0 \le sg_l(\bar{t}) \le S_l(t) < D_l(t) \tag{12}$$

$$sg_l(t') = 0, \ \forall t' \le t, \ D_l(t) \le S_l(t) \tag{13}$$

While the link inflow of a PC link is equal to the arrival flow, the link inflow of an SC link is given in Eq. (14), according to Eqs. (7)–(13).

$$r_a^{ml\hat{l}}(t) = \begin{cases} 0, & 0 \le S_l(t) < sg_l(\underline{t}) < D_l(t) \\ \sum_{\omega=\underline{t}}^{\bar{t}} u_a^{ml\hat{l}}(\omega), & 0 \le sg_l(\bar{t}) \le S_l(t) < D_l(t) \\ \sum_{\omega=\underline{t}}^{t} u_a^{ml\hat{l}}(\omega), & 0 \le D_l(t) \le S_l(t) \end{cases} \tag{14}$$

IVT of an SC link $a \in A_s^v$ can be expressed in a similar way as Eq. (2). Without considering parking costs, the link disutility of using SC is equivalent to the total disutility caused by waiting time, IVT and the rental costs under the dynamic pricing scheme, yielding

$$disU_a^{ml\hat{l}}(t) = \lambda_0^m \cdot t_a^{ml,w}(t) + \lambda_1^m \cdot t_a^{ml\hat{l}}(t') + \lambda_2^m \cdot \sum_{\omega=t'}^{t'+t_a^{ml\hat{l}}(t')} \tau_a^{l,c}(\omega), \ a \in A_s^v \tag{15}$$

where t' equals to $t + t_a^{ml,w}(t)$ and $\tau_a^{l,c}(\omega)$ is the time-dependent rental cost for using SC during interval ω at l. This specification is different from Jorge et al. (2015), in which the rental cost was linear with IVT and only dependent on travelers' departure time. If the charge during peak-time is higher than during non-peak times, it is unfair for travelers who start traveling in peak-times and mostly travel during non-peak times. The rental price in this study is associated with the in-vehicle period and pick-up location.

4.2. Disutility of activity links

Following Ettema et al. (2007), the utility of conducting an activity in this study is dependent on the activity location, timing, and duration. The disutility of an episode of activity participation is defined as the gap between the ideal utility and the actual realization of arrival time, location, and duration. The disutility of conducting an activity (through activity link a) for class m arriving at location l at interval t, $disU_a^{ml\hat{l}}(t)$, is expressed as

$$disU_a^{ml\hat{l}}(t) = U_a^{m*} - U_a^{ml\hat{l}}\left(t, d_a^{ml}, \ c_a^{l\hat{l}}\right), \ a \in A^a \tag{16}$$

where U_a^{m*} is the ideal utility for conducting the activity. $U_a^{ml\hat{l}}(t, d_a^{ml}, c_a^{l\hat{l}})$ is the actual utility associated with timing t duration d_a^{ml} and capacity $c_a^{l\hat{l}}$ at activity location l, which is specified in a similar way as Liao (2016) as follows

$$U_a^{ml\hat{l}}\left(t, d_a^{ml}, \ c_a^{l\hat{l}}\right) = F_a^{ml}(t) \cdot \frac{\log\left(1 + \beta_a d_a^{ml}\right)}{\Phi\left(t, c_a^{l\hat{l}}\right)}, \ a \in A^a \tag{17}$$

$$\Phi\left(t, c_a^{l\hat{l}}\right) = \left(1 + \max(0, \ \frac{\sum_m u_a^{ml\hat{l}}(t) - \vartheta^m \cdot c_a^{l\hat{l}}}{c_a^{l\hat{l}}})\right)^{\gamma_a} \tag{18}$$

where $F_a^{ml}(t)$ is the coefficient for time dependency and defined as a quadratic function to obtain one to two time-dependent peaks, *log*-shape describes the relationship between utility and activity duration, and β_a is a re-scaling factor. $c_a^{l\hat{l}}$ is the capacity of the location. ϑ^m is the crowding perception of class m. If the total flow at the activity location exceeds $\vartheta^m \cdot c_a^{l\hat{l}}$, travelers will experience discomfort, the disutility of conducting the activity will be higher. $\gamma_a = 0$ means that congestion at the locations is not considered. The disutility function indicates location attractiveness across different timing, duration and flow.

4.3. Disutility of parking

Using PC possibly involves parking costs, which are determined by where, when and for how long it is parked. In an ATP, there may be multiple parking episodes. The duration of each is the time difference between when the car is parked and picked-up. Let $t(\hat{l}^s)$ and $t(\hat{l}^e)$ denote the times of parking and picking-up of a parking episode at location $\hat{l}$ respectively. The parking disutility is defined as follows

$$disU_a^{ml\hat{l},r}(t) = \lambda_2^m \cdot \sum_{\omega=t(\hat{l}^s)}^{t(\hat{l}^e)} \tau_a^{\hat{l},r}(\omega),\ t(\hat{l}^s) = t,\ a \in A_c^v \tag{19}$$

where $\tau_a^{\hat{l},r}(\omega)$ is the time-dependent parking cost per interval during ω at $\hat{l}$. Thus, the total parking disutility of an ATP is the summation of those disutilities across all the parking episodes.

Parking SC involves the choice of parking location and successive use after parking. If a traveler does not choose successively use at the end of a trip, parking cost is determined by who should pay, and where and for how long the SC is parked. Given the complexity and flexibility of parking an SC, there is no regulated parking tariff thus far. A utility function for parking SC is given in Balac et al. (2017), but how long a traveler should pay is not discussed. To investigate how parking cost should be paid, two parking scenarios are proposed in this section without considering the choice of successive use, which will be discussed in Section 6.2.

4.3.1. Parking scenario 1: the car-sharing operator pays the parking costs

This scenario supposes the costs for parking SC are paid by the car-sharing operator, which is the current practice in many car-sharing programs. The parking disutility for users is simply specified as

$$disU_a^{ml\hat{l},r}(t) = 0,\ a \in A_s^v \tag{20}$$

However, the car-sharing operator incurs parking costs on behalf of the users. The total parking costs of the operator concern how many SCs are parked at which time intervals and locations. These values can be conveniently derived from the dynamic stock.

4.3.2. Parking scenario 2: the users pay location-based parking costs

In this scenario, travelers pay a base cost for parking. The parking duration is not considered because it is difficult to track the trajectory of each SC from the aggregate flow. Thus, the disutility of parking depends only on the specific parking location,

$$disU_a^{ml\hat{l},r}(t) = \lambda_2^m \cdot \sum_{\omega=t}^{t+t_a^{\hat{l}B}} \tau_a^{\hat{l},r}(\omega),\ a \in A_s^v \tag{21}$$

where $t_a^{\hat{l}B}$ is a presumed fixed base parking duration at location $\hat{l}$.

4.4. Disutility of an ATP

The disutility of an ATP is calculated by aggregating the associated disutilities of activity-travel and parking. Under parking scenario 1, the ATP disutility of travelers who depart from h during k via path p is as follows

$$PU_{hp}^m(k) = \sum_{a\in A}\sum_t \delta_{at}^{hpk} \cdot disU_a^{ml\hat{l}}(t) + \sum_{a\in A_c^v}\sum_t \delta_{at}^{hpk} \cdot disU_a^{ml\hat{l},r}(t) \tag{22}$$

where δ_{at}^{hpk} is a 0–1 indicator variable, $\delta_{at}^{hpk} = 1$ if travelers depart from h via path p during k and arrive at link a during t; $\delta_{at}^{hpk} = 0$, otherwise.

Likewise, under parking scenario 2, using $\underline{PU}_{hp}^m(k)$ to denote the right side of Eq. (22), the ATP disutility is re-defined as

$$PU_{hp}^m(k) = \underline{PU}_{hp}^m(k) + \sum_{a\in A_s^v}\sum_t \delta_{at}^{hpk} \cdot disU_a^{ml\hat{l},r}(t) \tag{23}$$

5. Tolerance-based multi-class activity-based DUE

5.1. Formulation

After incorporating FFC, a multi-class activity-based DUE model is formulated. The classic DUE postulates that a traveler of any class departing from home during any period cannot get a lower ATP disutility by unilaterally adapting her/his ATP. That means, at a user equilibrium state, all utilized ATPs have equal and no higher disutility than all unutilized ATPs. This

study applies a broader definition of activity-based DUE by adding a tolerance component Szeto and Lo, 2006). This relaxation incorporates a degree of bounded rationality reflecting the fact that travelers may not necessarily choose the least disutility route and instead a minor tolerance is acceptable practically (Simon, 1955; Conlisk, 1996; Hensher, 2010). The equilibrium state with tolerance is formulated as Eq. (24), which is reduced to the classic DUE when $\varepsilon = 0$ (ε is the tolerance level, $\varepsilon \geq 0$). Although ε can be refined to specific classes and O-D pairs, we adopt a general term representing the average level. For completeness, the flow conservation constraints and flow propagation in a dynamic system are expressed as Eq. (25)–(32). In case that link travel time may not be integral, linear interpolation is adopted (Liu et al., 2015). The equivalent variational inequality problem in the discrete-time domain is formulated as Eq. (33). Therefore, the tolerance-based multi-class activity-based DUE encompasses all the choice facets of conducting complete activity programs.

$$\begin{cases} PU_{hp}^{m}(k) \leq (1+\varepsilon)\cdot \min\left\{PU_{hp}^{m}(k)\right\}, & \text{if } f_{hp}^{m}(k) > 0 \\ PU_{hp}^{m}(k) \geq (1+\varepsilon)\cdot \min\left\{PU_{hp}^{m}(k)\right\}, & \text{if } f_{hp}^{m}(k) = 0 \end{cases}, \forall m, h, p, k \tag{24}$$

$$\sum_{m}\sum_{h}\sum_{p}\sum_{k} f_{hp}^{m}(k) = \sum_{m} Q^{m} \tag{25}$$

$$u_{a}^{ml\hat{l}}(t) = \sum_{h}\sum_{p}\sum_{k} \delta_{at}^{hpk}\cdot f_{hp}^{m}(k) \tag{26}$$

$$\sum_{l} S_{l}(0) = Q^{sc} \tag{27}$$

$$\sum_{a,\hat{l}} v_{a}^{m\hat{l}l}(t) = \sum_{a',l'} u_{a'}^{mll'}(t) \tag{28}$$

$$f_{hp}^{m}(k) \geq 0 \tag{29}$$

$$u_{a}^{ml\hat{l}}(t) = v_{a}^{ml\hat{l}}\left(t + d_{a}^{ml}(t)\right), \ \forall a \in A^{a} \tag{30}$$

$$u_{a}^{ml\hat{l}}(t) = v_{a}^{ml\hat{l}}\left(t + t_{a}^{ml\hat{l}}(t)\right), \ \forall a \in A_{c}^{v} \tag{31}$$

$$x_{y(a)}^{l\hat{l}}(t) = \max\left(0, \ x_{y(a)}^{l\hat{l}}(t-1) + \sum_{m} u_{a\in A_{c}^{v}}^{ml\hat{l}}(t) + \sum_{m} r_{a'\in A_{s}^{v}}^{ml\hat{l}}(t) - c_{a}^{l\hat{l}}\right), \ y(a) = y\left(a'\right) \tag{32}$$

$$\sum_{m}\sum_{h}\sum_{p}\sum_{k} \max\left\{PU_{hp}^{m*}(k), (1+\varepsilon)\cdot \min\left\{PU_{hp}^{m*}(k)\right\}\right\}\cdot\left(f_{hp}^{m}(k) - f_{hp}^{m*}(k)\right) \geq 0 \tag{33}$$

where Q^{sc} is the total supply of SCs, $f_{hp}^{m^*}(k)$ is the path flow of class m departing from h and choosing ATP p during k at equilibrium with tolerance, and correspondingly $PU_{hp}^{m^*}(k)$ is the ATP disutility incurred by the travelers.

5.2. Solution algorithm

Provided that the relevant ATPs are explicitly represented, we adopt the path-flow swapping mechanism (Nagurney and Zhang, 1997) to solve the tolerance-based multi-class activity-based DUE model. The mechanism has a property of forced convergence to a stopping criterion by iterative path-flow adjustments. Similar procedures have been extensively applied (Huang and Lam, 2002; Szeto and Lo, 2006; Ramadurai and Ukkusuri, 2010; Liu et al., 2015). As also found, the convergence-checking gap values fluctuate along with the flow adjustment process due to time discretization. Although this effect can somehow be alleviated by manipulating link travel times, the supply-demand interactions of SCs add complexity to the flow adjustment process. The imbalance of supply and demand is likely to appear in the iterative process, which causes unsmooth ATP disutilities. Therefore, attaching tolerance to the activity-based DUE framework does not only reflect the bounded rational activity-travel behavior evidenced by real-world observations but also smoothens the adjustment process.

As the time dimension is discretized in the dynamic system, the mapping functions of ATP time and disutility may not be continuous with ATP flow. Thus, it is difficult to get a unique solution even without the indifference band. The existence of indifference band brought by tolerance further confirm the fact (Szeto and Lo, 2006; Di et al., 2015). It also implies a rethought of the existence and usefulness of unique equilibrium state, on which the previous studies have heavily drawn. Therefore, stable solutions still warrant the usefulness of this approach. To that effect, we claim the achieved dynamic equilibrium states are simulated. The analysis of the theoretic properties of the solutions is beyond the scope of the current study (we refer the readers to Mounce and Carey, 2011 and Ye and Yang, 2017).

The solution algorithm starts with initialized flows on the feasible ATPs and available SCs at the locations. The ATP disutility are calculated based on $\{f_{hp}^m(k)\}$, $S_l(t)$, $sk_l(t)$, $D_l(t)$ and $sg_l(t)$. Iteratively, ATP flows are adjusted and ATP disutilities are updated until the stopping criterion is met. The detailed steps are described as follows.

Step 0: *Initialization*. Set up the parameters and load the multi-state supernetworks for all activity programs. Initialize travel demand $\{Q^m\}$, fleet size Q^{sc}, initial supply $\{S_l(0)\}$, and an initial solution $\{f_{hp}^m(k)\}$ by averaging $\{Q^m\}$ on all the ATPs. Iteration counter n is set as 1;

Step 1: *Calculation*. Calculate $S_l(t)$, $D_l(t)$, $sk_l(t)$ and $sg_l(t)$ based on Eqs. (8)–(11) and obtain the actual traffic link arrival flow, inflow and queues based on Eqs. (26)–(32); then, calculate link and ATP disutilities based on Eqs. (1)–(7) and Eqs. (15)–(23).

Step 2: *Convergence check*. Let $\boldsymbol{\gamma}^n$ and $\mathbf{PU^n}$ denote the vectors of traffic flow indicator $\{\gamma_{hp}^m(k)^n\}$ and ATP disutility $\{PU_{hp}^m(k)^n\}$ at iteration n respectively. $\gamma_{hp}^m(k)^n$ is 1 if the flow of m on path p departing during k is significantly larger than zero, and 0 otherwise. If the following convergence condition

$$\max\left(\boldsymbol{\gamma}^{\boldsymbol{n}} \cdot \left(\mathbf{PU^n} - PU^{*\boldsymbol{n}}\right)\right) \le \varepsilon \cdot PU^{*\boldsymbol{n}} \tag{34}$$

is satisfied, the algorithm stops, where PU^{*n} is the minimum ATP disutility at iteration n. The current time-dependent ATP flows are considered at a simulated DUE state with tolerance; otherwise, continue.

Step 3: *Update*. Update ATP flows and reset the distributions of SCs.

Step 3.1: *Update current traffic flows*. Calculate

$$\mathbf{f}^{\boldsymbol{n}+1} = \begin{cases} \max\left(0, \mathbf{f^n} - \rho^n \cdot \mathbf{f^n} \cdot (\mathbf{PU^n} - PU^{*\boldsymbol{n}})\right), & \text{if } h,p,k \notin \Gamma^n \\ \mathbf{f^n} + \frac{\sum_{h,p,k \notin \Gamma^n} (\mathbf{f^n} - \mathbf{f^{n+1}})}{|\Gamma^n|}, & \text{if } h,p,k \in \Gamma^n \end{cases} \tag{35}$$

where $\mathbf{f}^n$ is the ATP flow vector at iteration n, $\Gamma^n = \{h,p,k:\ PU_{hp}^m(k)^n \le (1+\varepsilon)\cdot PU^{*\boldsymbol{n}}\}$, and $\rho^n = \rho^0/(\frac{n}{\mu^0})$. ρ^0 and μ^0 are given as flow adjustment parameters.

Step 3.2: *Return*. $S_l(t)$, $D_l(t)$, $sk_l(t)$ and $sg_l(t)$ are reset to the initial values. Set $n = n+1$ and return to Step 1. The proposed model achieves the tolerance-based equilibrium states through path-flow swapping procedure given that the fleet size and initial distribution of SCs are considered exogenous inputs. At any intermediate iteration during the path-flow adjustment process, the spatial distribution of SCs at the end of the day may be different from the initial setting. Thus, resetting the initial distribution of SCs at the next iteration of path-flow adjustment is needed.

During the path-flow adjustment process, the manipulated conditions, namely, $\lim_{n\to\infty} \rho^n = 0$, $\lim_{n\to\infty} \rho^n \cdot f_{hp}^m(k)^n = 0$ and $\sum_n \rho^n \cdot f_{hp}^m(k)^n = +\infty$ (Nagurney and Zhang, 1997; Huang and Lam, 2002) hold and channel the process to an convergence state with tolerance.

5.3. Discussion of parameter estimation

Parameter estimation relates to the two sides of any full-fledged activity-based models. On the one hand, these models seek integrity and high policy-sensitivity; on the other hand, they require consistent parameter settings about various activity-travel components. Thus far, no estimation work has directly linked to the proposed model as empirical work usually comes after the modeling counterpart. However, according to the literature, we find that building an estimation framework concerning the suggested model is feasible by combining revealed choice data (activity-travel diaries/trajectories) and stated choice surveys (especially for free-floating SC). Essentially, the parameter setting in this study is related to disaggregate activity-travel link disutilities of the travelers and aggregate system-wide conditions of the transport networks and facilities of locations.

For the link and path disutility functions related to travel by traditional transport modes and activity participation, revealed preference data should be collected for the estimation of parameters including value of in-vehicle/waiting time, value of monetary cost for parking and taking PT, the crowding effects at the locations, tolerance rate, and heterogeneities among the travelers. There is an existing estimation framework so-called recursive choice model or dynamic discrete choice model (Fosgerau et al., 2013) dedicated to route choice behavior at multiple stages. For travel link disutilities using SC, considering it's not yet in widespread use, the stated choice survey should be collected for the estimation of travel preferences opposed to other traditional transport modes. Recently, there have been some studies for that purpose (e.g., Kim et al., 2017). As revealed preference data and stated choices may refer to different groups of social-demographic background and hold different levels of error variances, the estimates should be scaled in an integrative estimation framework (Whitehead et al., 2012). Also, the calibration framework proposed by Gkiotsalitis and Stathopoulos (2016) allows us to obtain accurate system-wide parameters using activity-travel trajectories collected by GPS devices.

Taking together, we argue that parameters of the suggested activity-based DUE are estimable by integrating the state-of-the-art estimation techniques.

6. Numerical examples

In this section, three numerical examples are carried out to illustrate the proposed model. As formulated, the activity-based DUE takes into account multi-class travelers and heterogeneity. All parameters regarding activity-travel preferences

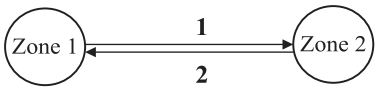

Fig. 5. Example 1.

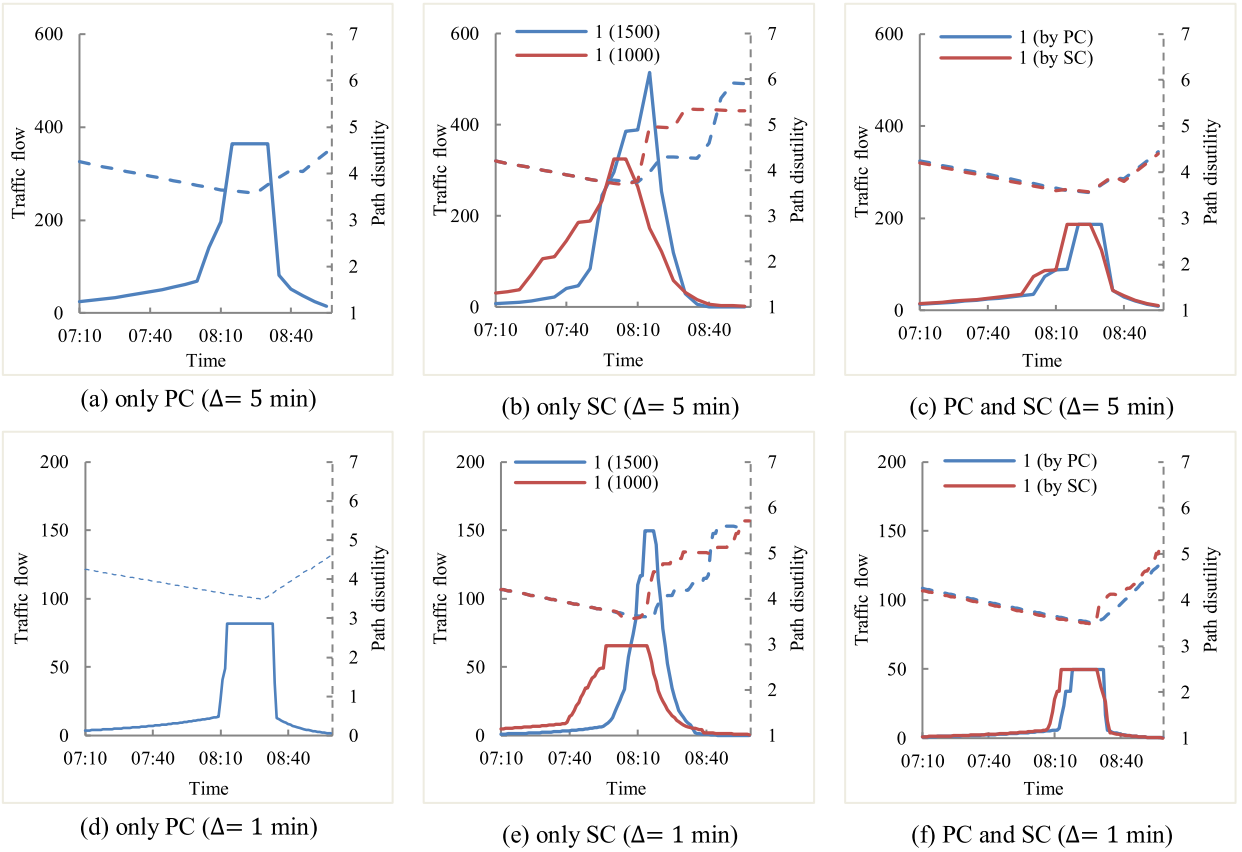

Fig. 6. Solution results.

from the traveler side need to be estimated and may be turned into latent and heterogeneous for capturing specific groups of travelers. The system-wide conditions are in general exogenous variables and homogenous to the travelers that cover travel link BPR functions, SC supply settings, and attributes of locations of facilities.

The solution algorithm is coded in MATLAB and run on a personal computer with Intel Core™ i7- CPU of 3.4 GHz and 16 GB RAM. For different illustration purposes, the network scales are set in an accumulative way with ordinary ATPs explicitly identified. Note that methods for generating personalized networks and ATPs (Liao et al., 2011; Liao and van Wee, 2016) should be applied for real-world applications.

6.1. Example 1

To illustrate the supply-demand interactions of SCs, we first consider a simple example that only includes two OD pairs for bi-directed morning commuting trips between zone 1and 2 Fig. 5). Suppose $Q^m = 2500$ ($m = 1$, only one class) for each OD pair and the travel links ($a = 1, 2$) are homogeneous with $t_a^0 = 30$ min, $c_a^{12} = 50$ veh/min, $\eta_a = 0.02$ and $\gamma_a = 1$ in Eq. (2). Following the tradition of one bottleneck-based DUE, the linear penalty of arriving early and late for commuting trips is adopted, which is a special case of the timing dependency of Eqs. (16)–(18). Suppose further the start time of work is 9:00 a.m., and the penalty of arriving early and late is 0.01 and 0.04 unit of disutility/min respectively. The departure time range is taken from 6:00 a.m. to 10:00 a.m. Other parameters are set as $\lambda_0^m = 0.002$ and $\lambda_1^m = 0.1$ unit of disutility/min, $\lambda_2^m = 0.15$ unit of disutility/€,$\tau_a = 0.1$ and $\tau_a^{l,c}(t) = 0.09$ e/min $\forall t$ for using PC and SC respectively, $\rho^0 = 5$, and $\mu^0 = 100$ (see Section 3.2 for definitions of notations).

Fig. 6 presents the choice of departure time and mode at the equilibrium states under three situations (i.e., using PC only, SC only, and both) of different time intervals ($\Delta = 5$ min and $\Delta = 1$ min). For better representations of the traffic flow

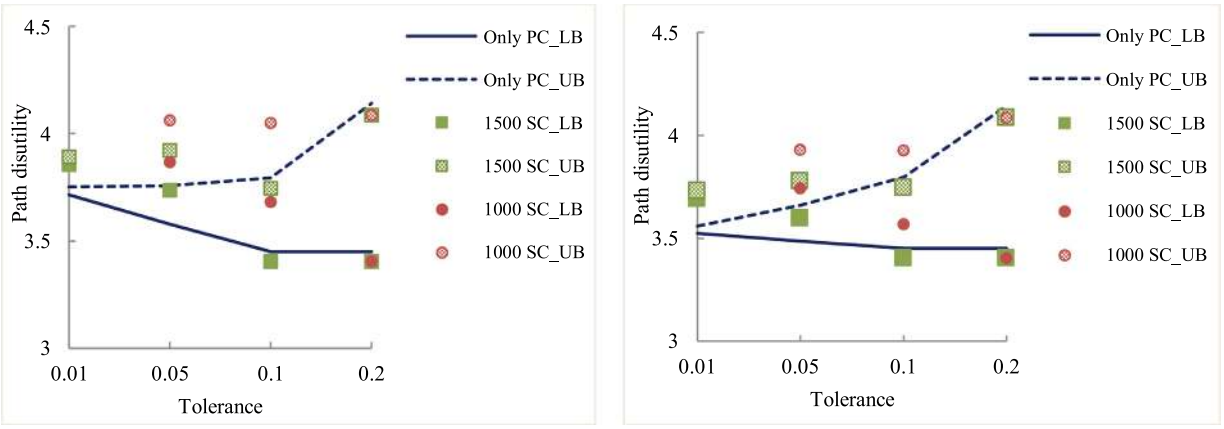

Fig. 7. Sensitivity analysis of tolerance level and initial supply of SC.

distributions, the departure time ranges from 7:10 a.m.to 9:00 a.m. Only the flows and disutilities on link 1 are shown since the outcomes are symmetrical to link 2. ε is in general set as 0.05 or 0.1 for illustration purpose (according to Mahmassani and Liu, 1999, tolerance levels were empirically found within 0.2). The tolerance-based DUE states are achieved within 10 s and 32 s of CPU computation time when a time interval is 5 min and 1 min respectively.

As shown in Fig. 6(a) and (d), travelers adapt departure times within 8:10 a.m. and 8:30 a.m. to achieve equilibrium with the tolerance due to the penalty for arriving early and late. Fig. 6(b) and (e) show flow patterns when the initial supplies of SCs at each zone are 1500 ($\varepsilon = 0.05$) and 1000 ($\varepsilon = 0.1$) respectively. In the latter case, ε is set larger as the supply of SCs considerably decreases. It is because when SCs become deficient, travelers may have to increase tolerance to achieve new equilibrium. As seen, when fewer SCs are supplied, travelers incur waiting for SCs coming from the other zone and thus some travelers choose to depart earlier. Fig. 6(c, f) show the results of the third situation ($\varepsilon = 0.05$) with 1000 SCs initially supplied at each zone besides the availability of PC. As using SC is set slightly cheaper, travelers choose SCs on the condition of no waiting and approximately half choose PC to avoid to waiting. Low time resolution (e.g., 5 min) of the discrete time domain means travelers tend to wait long for the SCs being replenished if there is a deficient stock, which may require a higher tolerance for reaching the equilibrium state. With a higher time resolution (e.g., 1 min), more travelers avoid unnecessary waiting. As shown in subfigures (b, e), the flow distributions of 1-minute resolution are smoother than those of 5-minute under the same tolerance rate. However, as shown in subfigures (c, f), the issue is partly remedied when the travelers have both PC and SC as mode alternatives. It means travelers still utilize SCs sufficiently in complementation with PCs by adjusting their departure times.

Fig. 7 shows the lower bound (LB, PU^*) and upper bound (UB, $(1+\varepsilon)\cdot PU^*$) of ATP disutility at equilibrium with different settings of Δ, tolerance, and initial supply of SCs. In line with the sensitivity analysis in Szeto and Lo (2006), it shows that the equilibrium solutions are influenced by ε. The solid and dash line indicate the LB and UB of ATP disutility respectively at the equilibrium states of using PC only. Under a certain tolerance, if the UB of ATP disutility of using SC lies within the ATP disutility range ([LB, UB]) of using PC, it can be inferred that 2500 PCs may be replaced by fewer SCs. As illustrated in Fig. 7 (a, b), 2500 PCs may be replaced by 1500 SCs when ε is 0.1, and by 1000 SCs when ε is 0.2.

6.2. Example 2

Three test scenarios are considered to illustrate the choice of ATP and the evolution of supply-demand of SCs in a simple network (Fig. 8). The first scenario consists of transport modes of PC and SC, PT is added in the second scenario, and the third further includes the successive use of SC for trip chains. The time horizon is set from 6:00 a.m.to 22:00 pm and travelers may depart from home between 6:00 a.m.and 10:00 a.m.to conduct two daily activities (work and shopping). Travelers are equally divided into two classes by whether they have the membership of FFC ($m = 1$ if owning membership; otherwise, $m = 2$). The purpose is to examine the influence of SCs on the demand responses. General parameters are set as $\Delta = 5$ min, $\varepsilon = 0.05$, and $\gamma_a = 0$ for activity links in Eqn. (18).

6.2.1. Scenario 1: PC + SC

Suppose shopping has two duration options for simplicity. Besides travel links numbered from 1 to 10, link 11 represents working, links 12–13 and 14–15 shopping at location S_1 and S_2 with two durations (30 min or 60 min) respectively. By considering an activity chain 'H-W-S_1/S_2–H', there are eight ATPs for the travelers with FFC membership and four feasible ATPs otherwise. 12 ATPs are numerated by pre-defined activity-travel chains in Table 3. $Q^1 = Q^2 = 2500$ at H, $\vartheta^1 = \vartheta^2 = 0.5$, $S_H(0) = 1500$ (initial supplies at other locations are 0). The first class of travelers has 8 ATPs for shopping at two locations by

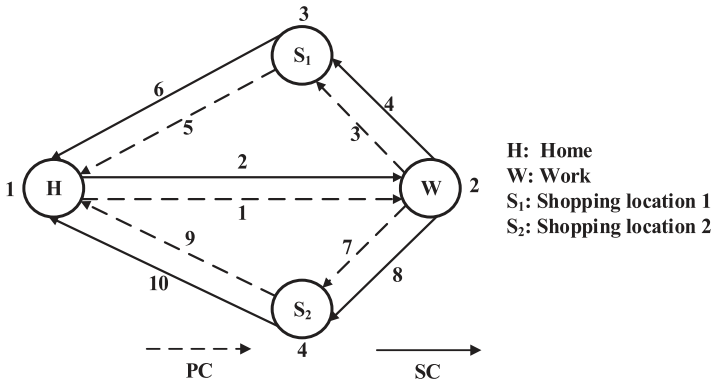

Fig. 8. Example network for Scenario 1.

Table 3
Feasible ATPs.

Class	ATP number	Link order					Activity pattern	Mode combination
		1st	2nd	3rd	4th	5th		
1	1–2	1	11	3	12/13	5	H-W-S_1-H	PC - PC - PC
	3–4	2	11	4	12/13	6		SC - SC - SC
	5–6	1	11	7	14/15	9	H-W-S_2-H	PC - PC - PC
	7–8	2	11	8	14/15	10		SC - SC - SC
2	9–10	1	11	3	12/13	5	H-W-S_1-H	PC - PC - PC
	11–12	1	11	7	14/15	9	H-W-S_2-H	

Table 4
Parameter settings.

Travel links	Link attributes				Nodes	Node attributes			
	time window (min)	t_a^0 (min)	η_a, γ_a	$c_a^{\hat{l}}$ (/min)		$\tau_a^{l,r}(t)^*$ (€/min)		$\tau_a^{l,c}(t)$ * (€/min)	
1–10	[360, 1320]	30	0.15, 1	100	1/2	0		0.15	
Activity links	time window (min)	U_a^{m*}	β_a	d_a^{ml} (min)	3/4	0		0.15	
11	[540, 1320]	20	1	480	Class	λ_0^m (/min)	λ_1^m (/min)	λ_2^m (/€)	τ_a (€/min)
12–15	[540, 1320]	10	1	30, 60	1/2	0.2	0.1	0.1	0.15

PC and SC, while the second has 4 ATPs for shopping at S_1 and S_2 by PC. Parameter settings for travel, parking, and activity are shown in Table 4. The quadratic function (Eq. (17)) is defined as $-0.001(t-7.5)(t-8)(t-17)(t-18)+1$ for working and $-0.001(t-7.5)(t-8)(t-18)(t-19)+1$ for shopping at S_1 and $-0.002(t-7.5)(t-8)(t-18)(t-19)+1$ at S_2, which have different preferences for activity timing.

Fig. 9(a–c) show the evolution of supply-demand of SCs at the locations and the time-dependent ATP flows at the equilibrium state with tolerance. As seen, the supply at H gradually shifts to W because a large amount of travelers take SC to work (Fig. 9(a)), in opposition to the demand dynamics (Fig. 9(c)). This supply-demand interaction resembles those in circumstances when travelers leave W for shopping, and all SCs are returned to H at the end of the day. Note that not all SCs are utilized. As shown by the ATP flows in Fig. 9(b), nearly all travelers choose shopping for one hour, since it causes lower disutility than shopping for 0.5 h at either S_1 or S_2 given that the timing for shopping is confined to the time zone after work. Both S_1 and S_2 attract travelers for avoiding congestion on the shopping trips. Since S_1 is set more attractive than S_2, flows on ATP 2 by PC and ATP 4 by SC are larger than those on ATP 6 and 8 (travelers of $m=1$), and more travelers choose ATP 10 than ATP 12 (travelers of $m=2$).

Fig. 9(d) presents the sensitivity analysis on the effects of combined rental price and fleet size on the usage of SC at H. With each combination of setting, the simulated equilibrium state is achieved within 600 iterations of flow adjustment within 100 s CPU computation time on average. It shows that with the same fleet size, the higher the rental price, the fewer travelers choose SC. Given a rental price, likewise, the more fleet size, the more travelers choose SC when the price is lower than 0.2 €/min. When the price is 0.2 €/min, there is no further more usage of SC even if the fleet size increases, implying an upper bound usage at a particular high rental price. As shown, the proposed model is capable of capturing the dynamic process of using SCs, which are influenced by the fleet size and rental price from the supply side.

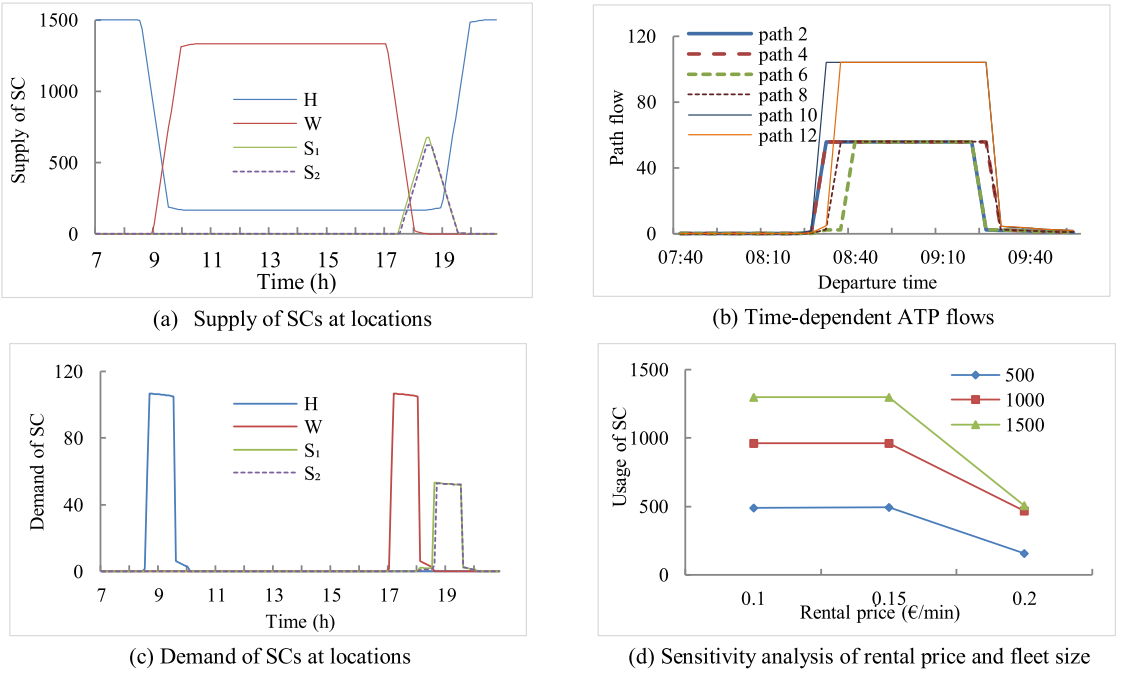

(a) Supply of SCs at locations

(b) Time-dependent ATP flows

(c) Demand of SCs at locations

(d) Sensitivity analysis of rental price and fleet size

Fig. 9. Solution results.

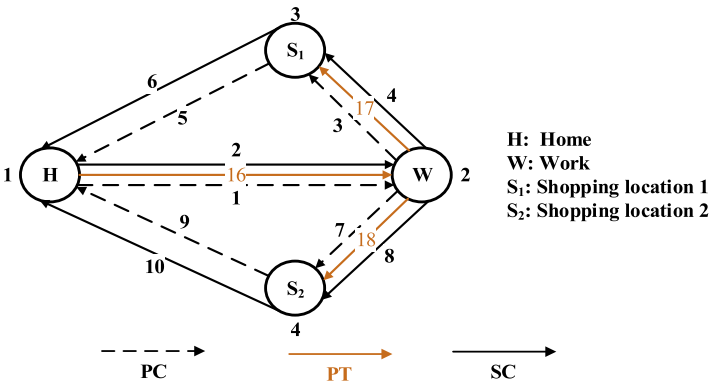

Fig. 10. Example network for Scenario 2.

Table 5
Feasible ATPs.

Class	ATP number	Link order					Activity pattern	Mode combination
		1st	2nd	3rd	4th	5th		
1	13–14	2	11	17	12/13	6	H-W-S_1-H	SC - PT - SC
	15–16	16	11	17	12/13	6		PT - PT - SC
	17–18	16	11	4	12/13	6		PT - SC - SC
	19–20	2	11	18	14/15	10	H-W-S_2–H	SC - PT - SC
	21–22	16	11	18	14/15	10		PT - PT - SC
	23–24	16	11	8	14/15	10		PT - SC - SC

6.2.2. Scenario 2: PC + SC + PT

Based on scenario 1, this scenario adds three PT lines (Fig. 10) to study the effect of modal substitution and trip chaining with SC. With this purpose, travelers without membership of FFC are not considered ($Q^1 = 2500$ and $Q^2 = 0$). By removing ATP 9–12, the added feasible ATPs are numerated in Table 5. For each PT line, the capacity is 200 per vehicle with a frequency of 15 min, the free flow IVT is 35 min, and η_a, γ_a, and ϑ^1 in Eq. (5) are set as 0.15, 4, and 0.5 respectively. The

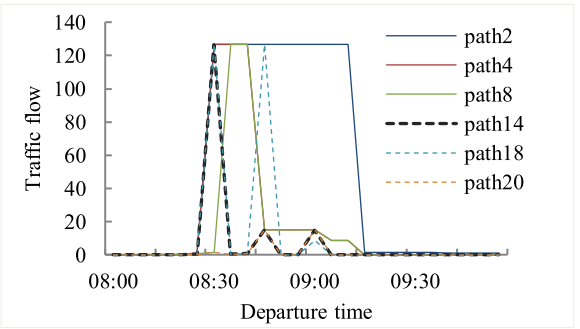

(a) ATP inflow

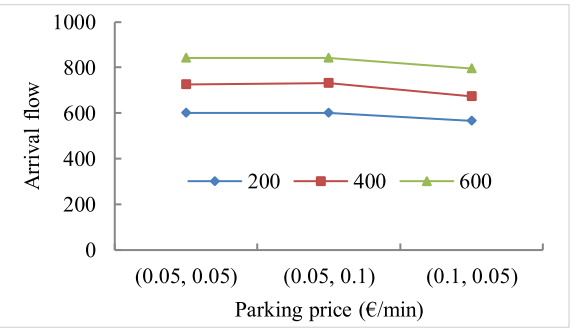

(b) Arrival flow at S1

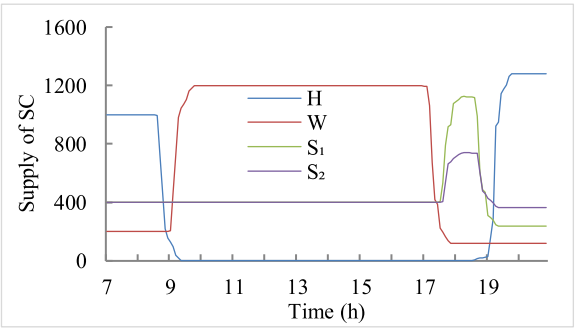

(c) Supply of SCs at the locations

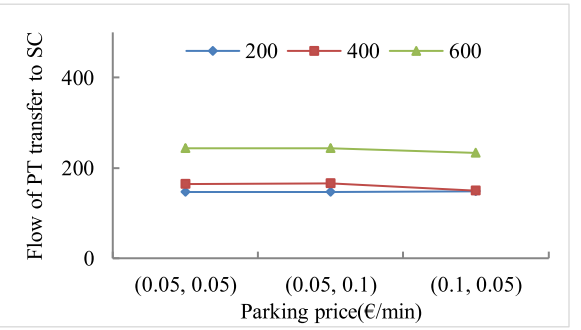

(d) Transfer flow at S_1

Fig. 11. Sensitivity analysis of distribution and parking price.

parking prices for PC are 0.1 and 0.05 €/min at S_1 and S_2, and the base parking costs for SC are € 0.5 and € 0.25 at S_1 and S_2, respectively. Initial supplies are redistributed as: $S_H(0)=1000$, $S_W(0)=200$, $S_{S_1}(0)=400$ and $S_{S_2}(0)=400$.

Fig. 11(a, c) depict the resultant time-dependent ATP flows and the evolution of supply of SCs respectively. These dynamics are consistent with each other. In particular, due to the penalty for waiting PT, flows on ATP 14, 18 and 20 (trips with PT denoted by dashed lines in Fig. 11(a)) occur at the time when PT vehicles arrive. It means that PT does not only substitute PC or SC, but also forms trip chains with SC as indicated by the contents of the chosen ATPs. As travelers departing from home by PT are allowed to return home by SC, the final supply at H is higher than the initial. It is evidenced by the result that the supply at S_1 is lower than S_2, i.e., more travelers visit S_1 and some first take PT and then SC.

Fig. 11(b, d) show the results of sensitivity analysis on the combination of parking price and distribution of SC at S_1 and S_2. The horizontal axis denotes the combination of parking price at S_1 and S_2 in €/min and the values in the legends represent the supply of SCs at S_1 with the total supply at S_1 and S_2 fixed as 800. The vertical axis in subfigure (b) denotes the arrival flow at S_1, which is the difference of the dynamic supply during the day and the initial supply, and in subfigure (d) the transfer flow from PT (for shopping) to SC (for returning home). Although the effects are not strong, it can be seen that the more fleet size at S_1, the more travelers choose S_1. It is because more travelers take PT to S_1, which decrease the queue on the road and decrease the ATP disutility. Moreover, it shows that higher parking costs discourage travelers from visiting S_1.

6.2.3. Scenario 3: successive use of SC

A traveler with FFC membership may consider the successive use of the same SC at the end of a car-sharing trip when the ensuing activity duration is short. When such a choice is made, the traveler will not experience waiting time when picking-up the SC. Besides, the SC will not contribute to the supply when it is parked and not generate the demand when the traveler picks it up. To consider this choice facet, the third scenario analysis is considered.

Let $a(\hat{l}\rightarrow l)$ and $a'(l'\rightarrow l'')$ be two SC links before and after an activity link $(l\rightarrow l')$, for which some SCs are locked for successive use. We define an indicator variable $\sigma_{at}^{hpk}=1$ if travelers who depart from h via p during k and arrive at l of a during t are in successive use of SC; $\sigma_{at}^{hpk}=0$, otherwise. The demand and supply of SCs are re-written as follows

$$D_{l'}(t')=\sum_m\sum_{a',\ l''}u_{a'}^{ml'l''}(t')-\sum_m\sum_h\sum_p\sum_k\sigma_{a't'}^{hpk}\cdot f_{hp}^m(k)+sg_{l'}(t'-1) \tag{36}$$

$$S_l(t)=\sum_m\sum_{a,\hat{l}}v_a^{m\hat{l}l}(t)-\sum_m\sum_h\sum_p\sum_k\sigma_{at}^{hpk}\cdot f_{hp}^m(k)+sk_{\ l}(t-1) \tag{37}$$

Table 6
Feasible ATPs.

Class	ATP number	Link order					Activity pattern	Mode combination
		1st	2nd	3rd	4th	5th		
1	3–4	2	11	4	12/13	6	H-W-S_0-H	SC - SC(successive) -SC
	13–14	16	11	4	12/13	6		PT - SC(successive) -SC
	15–16	2	11	18	14/15	10	H-W-S_0'-H	SC - PT - SC
	17–18	16	11	18	14/15	10		PT - PT - SC
	19–20	16	11	8	14/15	10		PT - SC - SC

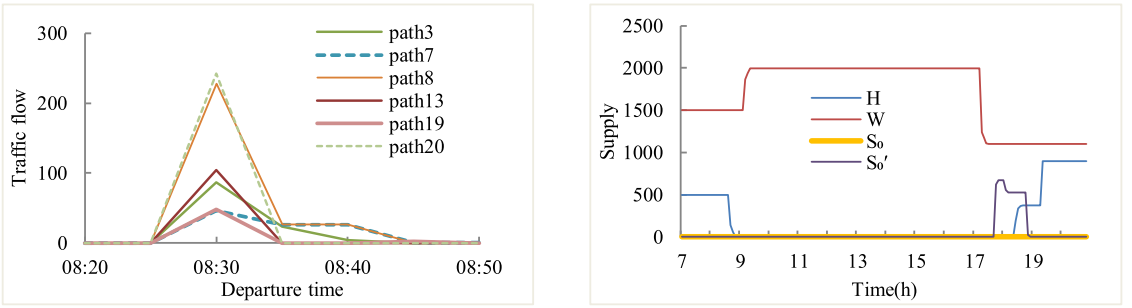

(a) Path flow (b) Supply of SC at the locations

Fig. 12. Equilibrium state with the consideration of successive use.

Eqs. (36) and (37) indicate that the demand and supply of SCs at the locations should neglect the travelers who have chosen successive use. The parking disutility of using SC with successive use is the same as using PC. Moreover, the waiting time $t_{a'}^{ml',w}(t)$ is equal to zero for those who are in successive of SC.

The network of Scenario 3 is the same as that in Scenario 2, but we redirect S_1 and S_2 as the same location and redefine them as S_0 and S_0' for travelers who choose and don't choose successive use respectively. Keeping the link and ATP numbers in Table 3 unchanged, several added feasible ATPs are numerated in Table 6. The shopping duration choices at S_0 (S_0') are 15 min and 60 min. The quadratic function for shopping is re-defined as $-0.01(t-7.5)(t-8)(t-18)(t-19)+0.1$, which decrease the difference of shopping disutility between two durations but enlarge the difference of different timing. The initial supplies of SCs are 1500 at H, 500 at W, and 0 at S_0 (S_0'). To enlarge the influence of parking cost, the parking price for both PC and SC is increased to 0.2 €/min. The other parameters are the same as those used in Scenario 1.

It can be observed in Fig. 12(a) that most travelers choose successive use for short shopping duration for pattern H-W-S_0–H, and most travelers choose ATP 3 and 13; while for pattern H-W-S_0'-H, most travelers choose ATP 8 and 20 for long shopping duration. It is because long shopping means more parking costs and ATP disutilities for both PC and successive use of SC, while less parking cost is required for non-successive SC. Fig. 12(b) shows the evolution of supply. As travelers take successive use of SC for shopping at S_0, there is no supply (and no demand by deduction) of SC at S_0.

6.3. Example 3

This example concerns a relatively large multimodal transport network (Fig. 13). The purpose is to test the model feasibility with the consideration of full-fledged choice of ATP, which entails choice of activity sequence/location/duration and route/mode, traveler heterogeneity, location capacity, and the evolution of supply-demand of SCs. The network is adapted from Nguyen–Dupuis network (Nguyen and Dupuis, 1984) and analogously divided to one city center and two suburban areas, where facilities of home (H), working (W), shopping (S) and entertainment (E) are distributed. ATPs are generated by rule of thumb: first, activity chains are generated for travelers living in H_1 and H_2 with the specification of activity sequence/location choice (see supplementary information (SI), Table S1); second, ATP skeletons are determined with the specification of mode choice (SI, Table S2); third, detailed ATPs are specified with route and duration choice (SI, Table S3) (nodes/locations and links are specified in Table S4-7). In total, 8 activity chains, 47 ATP skeletons, and 578 detailed ATPs are identified. The time horizon is set from 6:00 a.m.to 20:00 pm and travelers may depart from home between 6:00 a.m.and 10:00 a.m.to conduct daily activities (staying home, work, shopping, and entertainment). By setting $\Delta = 1$ min, there are 240 departure time choices and 138,720 time-dependent ATPs.

The traveler characteristics are set as follows: total travel demand $\sum_m Q^m = 50{,}000$, with 80% living at H_1 and 20% at H_2, 50% owning PC and 80% having working activity. Travelers are classified into 4 classes by their membership of FFC and valuation of time/money. There are 31 OD pairs, and 60%, 30% and 10% of working, shopping, and entertainment activities respectively (Table S8). The fleet size of SC is 20% of the total travel demand and the majorities are initially parked in the city center. Besides, traveler heterogeneity in terms of valuations of time/money is set in Table S9.

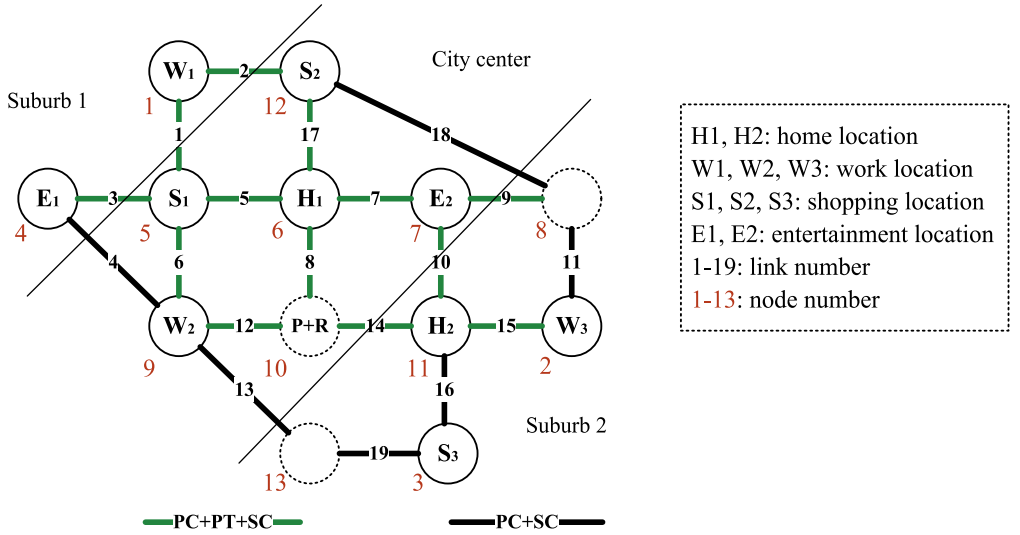

Fig. 13. Activity-based Nguyen–Dupuis network.

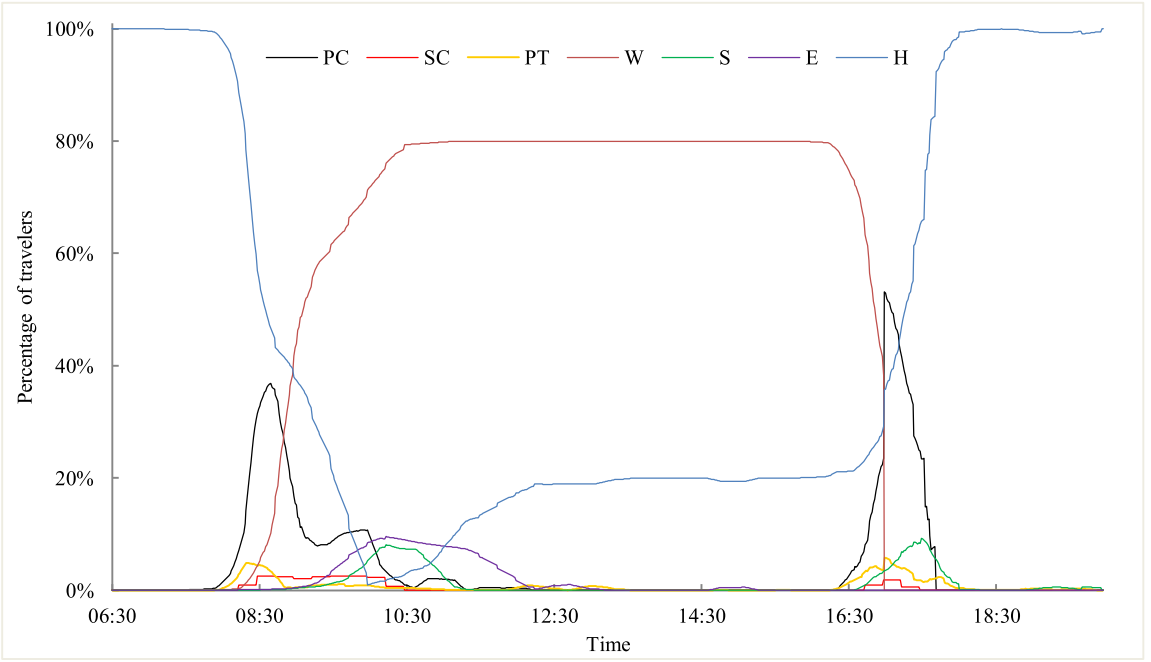

Fig. 14. Percentage of travelers on activity and travel links when $\varepsilon = 0.05$ and $\Delta = 1$ min.

When ε are set as 0.05, 0.1 and 0.15 respectively, the tolerance-based DUE states are all achieved within 600 s of CPU computation time, indicating the computational feasibility. The model system can entail all traveler choices and facility usages as shown above. Nevertheless, it is beyond the purpose of this example to show all the outcomes. At the aggregate level, we demonstrate the space-time distributions of travelers in the multimodal system when ε is 0.05. Fig. 14 shows the percentage of travelers on activity links (at the locations) and travel links (by specific transport modes). It demonstrates that non-work travelers depart later than commuters for avoiding traffic congestion and seeking better activity timing. In addition, most non-workers do shopping in the morning and entertainment in the afternoon depending on the utility specifications of activity participation. Flow distributions of travelers who live at H_2 have fewer varieties than those live at H_1 in terms of daily activity and mode choice set. Overall, it exhibits the space-time distribution of travelers in the multimodal system.

Fig. 15 shows the supplies of SCs at the locations when ε is 0.05, which also reflects the dynamic choice of SC and activity locations. Subgraph (a) shows that the use rate of SC at H_2 is marginally higher than at H_1 in the morning. In Subgraph (b),

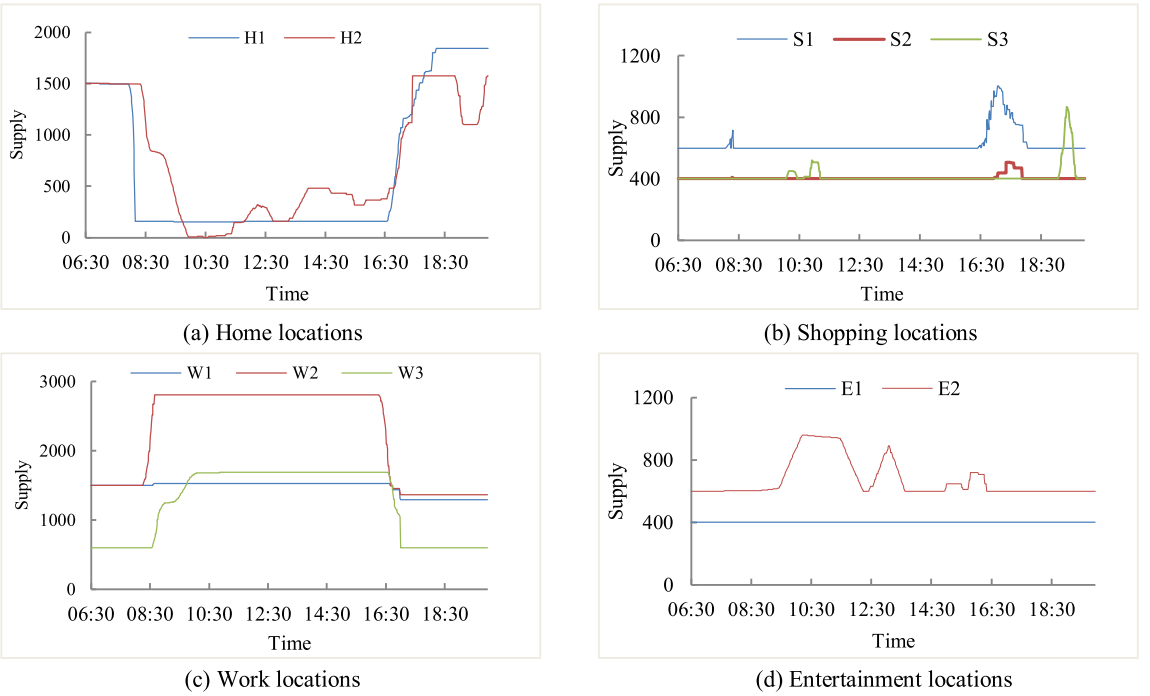

Fig. 15. Supply of SCs at the locations.

more travelers do shopping at S_1 than at S_2 by SC since the road capacity of link 5 and location capacity of S_1 are larger than those of link 17 and S_2 respectively. Thus, travelers choose S_1 can avoid traffic congestion and crowding. Subgraph (c, d) indicate that fewer travelers take SC to W_1 or E_1, which is mainly due to the longer travel time from H_1 to W_1 and E_1 that generate more rental costs of using SC. To test the stability of the solutions, we rerun the example with multiple random initializations of ATP flows. It is found that the space-time distributions of SCs are much similar to Fig. 14 but the ATP flows at the equilibrium states show higher variability. Nevertheless, the overall relative differences of the 578 ATP flows are less than 23%.

7. Conclusions and future work

Car-sharing systems especially FFC have recently attracted growing attention. Related studies have mostly focused on modeling operational management and user preferences. In addition to the microsimulation-based studies, this study incorporates FFC into an activity-based DUE via multi-state supernetworks and demonstrates the supply-demand interactions of SCs. The choice of an ATP through a multi-state supernetwork consists of the choice of departure time, route, mode, activity sequence, location, duration, and parking location. Travelers are divided into classes based on membership of FFC and valuation of time/money. The multi-class activity-based DUE model also considers traveler bounded rationality, which does not only incorporate the behavior evidenced by real-world observations but also speeds-up the path-flow adjustment process. Three numerical examples demonstrate the model capable of capturing the dynamic supply-demand interactions of SCs.

Although the proposed model offers a valuable way of analyzing the effects of FFC, several important components have not been considered in the proposed model. Several operational assumptions may be relaxed in future work. First, to relax assumption **A5**, a refined allocation mechanism should be developed for more efficiently managing the inventory of SCs. Second, the formulated problem is studied under a deterministic representation of the urban system; however, most travel components may be uncertain in reality. Notably, due to the uncertain travel time in the road network, the supply-demand interactions of SCs would be uncertain as well, resulting in uncertain waiting time for SCs. A model extension should consider the fact that travelers may have different risk attitudes about waiting time and IVT. Modeling travelers' choice behavior under such circumstances needs a reformulation of the problem. Third, the proposed model mainly addresses the dynamic process of SCs and travelers' ATP choices under the provision of car-sharing services. The system optimization of fleet size, autonomous vehicle relocation, and rental price has large implications for travel demand management. The next step is to link the activity-based DUE model to supply policies related to reservation and relocation strategies, day-to-day evolution mechanisms, and FFC service areas. Fourth, another limitation of the current study is that only one FFC service operator is considered given the purpose of studying user equilibrium. The extension to analyze competition between multiple service operators is also on our research agenda. Fifth, for real-world applications, the proposed model should also be linked to systemic estimation and calibration frameworks, the generation of travelers, activity programs and ATPs should be based on and

calibrated from activity-travel diaries, socio-demographic information, and policy scenarios. These issues will be addressed in our future research.

Acknowledgments

This work was jointly supported by the Netherlands Organization for Scientific Research(NWO), the National Natural Science Foundation of China (NSFC, Project No. 71361130011, 71371094) and the National Social Science Foundation of China (NSSFC, Project No. 16ZDA047).

Supplementary materials

Supplementary material associated with this article can be found, in the online version, at doi:10.1016/j.trb.2017.11.011.

References

Arentze, T.A., Timmermans, H.J.P., 2004. Multistate supernetwork approach to modelling multi-activity, multimodal trip chains. Int. J. Geogr. Inf. Sci. 18, 631–651.
Balac, M., Ciari, F., Axhausen, K.W., 2017. Modeling the impact of parking price policy on free-floating carsharing: case study for Zurich, Switzerland. Transp. Res. Part C 77, 207–225.
Bansal, P., Kockelman, K.M., Singh, A., 2016. Assessing public opinions of and interest in new vehicle technologies: an Austin perspective. Transp. Res. Part C 67, 1–14.
Barrios, J., Godier, J., 2014. Fleet sizing for flexible carsharing systems: simulation-based approach. Transp. Res. Rec. 2416, 1–9.
Boyacı, B., Zografos, K.G., Geroliminis, N., 2017. An integrated optimization-simulation framework for vehicle and personnel relocations of electric carsharing systems with reservations. Transp. Res. Part B 95, 214–237.
Cepolina, E.M., Farina, A., 2012. A new shared vehicle system for urban areas. Transp. Res. Part C 21 (1), 230–243.
Chow, J.Y.J, Djavadian, S., 2015. Activity-based market equilibrium for capacitated multimodal transport systems. Transp. Res. Part C 59, 2–18.
Childress, S., Nichols, B., Charlton, B., Coe, S., 2015. Using an activity-based model to explore the potential impacts of automated vehicles. Transp. Res. Rec. 2493, 99–106.
Ciari, F., Balac, M., Axhausen, K.W., 2016. Modeling carsharing with the agent-based simulation MATSim: state of the art, applications, and future developments. Transp. Res. Rec. 2564, 14–20.
Ciari, F., Schuessler, N., Axhausen, K.W., 2013. Estimation of carsharing demand using an activity-based microsimulation approach: model discussion and some results. Int. J. Sustainable Transp. 7 (1), 70–84.
Clemente, M., Fanti, M.P., Mangini, A.M., Ukovich, W., 2013. The vehicle relocation problem in car sharing systems: modeling and simulation in a petri net framework. In: Application and Theory of Petri Nets and Concurrency. Springer, Berlin Heidelberg, pp. 250–269.
Conlisk, J., 1996. Why bounded rationality? J. Econ. Literat. 34 (2), 669–700.
Di, X., Liu, H.X., Ban, X.J.X., Yu, J.W., 2015. On the stability of a boundedly rational day-to-day dynamic. Netw. Spatial Econ. 15 (3), 537–557.
Djavadian, S., Chow, J.Y.J., 2017. An agent-based day-to-day adjustment process for modeling 'mobility as a service' with a two-sided flexible transport market. Transp. Res. Part B 104, 36–57.
Ettema, D.F., Bastin, F., Polak, J., Ashiru, O., 2007. Modelling the joint choice of activity timing and duration. Transp. Res. Part A 41, 827–841.
Fosgerau, M., Frejinger, E., Karlström, A., 2013. A link based network route choice model with unrestricted choice set. Transp. Res. Part B 56, 70–80.
Fu, X., Lam, W.H.K., 2014. A network equilibrium approach for modelling activity-travel pattern scheduling problems in multi-modal transit networks with uncertainty. Transportation 41 (1), 37–55.
Garikapati, V.M., Pendyala, R.M., Morris, E.A., Mokhtarian, P.L., McDonald, N., 2016. Activity patterns, time use, and travel of millennials: a generation in transition? Transp. Rev. 36 (5), 558–584.
Gkiotsalitis, K., Stathopoulos, A., 2016. Joint leisure travel optimization with user-generated data via perceived utility maximization. Transp. Res. Part C 68, 532–548.
Heilig, M., Mallig, N., Schröder, O., Kagerbauer, M., Vortisch, P., 2017. Implementation of free-floating and station-based carsharing in an agent-based travel demand model. Travel Behav. Soc. Doi.org/10.1016/j.tbs.2017.02.002.
Hensher, D.A., 2010. Attribute processing, heuristics and preference construction in choice analysis. In: Hess, S., Daly, A. (Eds.), State-of Art and State-of Practice in Choice Modelling, pp. 35–70.
Hu, L., Liu, Y., 2016. Joint design of parking capacities and fleet size for one-way station-based carsharing systems with road congestion constraints. Transp. Res. Part B 93, 268–299.
Huang, H.J., Lam, W.H.K., 2002. Modeling and solving the dynamic user equilibrium route and departure time choice problem in network with queues. Transp. Res. Part B 36 (3), 253–273.
Jorge, D., Correia, G.H.D.A., 2013. Carsharing systems demand estimation and defined operations: a literature review. EJTIR 13 (3), 201–220.
Jorge, D., Molnar, G., Correia, G.H.D.A., 2015. Trip pricing of one-way station-based carsharing networks with zone and time of day price variations. Transp. Res. Part B 81, 461–482.
Kaspi, M., Raviv, T., Tzur, M., 2014. Parking reservation policies in one-way vehicle sharing systems. Transp. Res. Part B 62, 35–50.
Kaspi, M., Raviv, T., Tzur, M., Galili, H., 2016. Regulating vehicle sharing systems through parking reservation policies: analysis and performance bounds. Eur. J. Oper. Res. 251 (3), 969–987.
Kim, J., Rasouli, S., Timmermans, H.J.P., 2017. Satisfaction and uncertainty in car-sharing decisions: an integration of hybrid choice and random regret-based models. Transp. Res. Part A 95, 13–33.
Kopp, J., Gerike, R., Axhausen, K.W., 2015. Do sharing people behave differently? An empirical evaluation of the distinctive mobility patterns of free-floating car-sharing members. Transportation 42 (3), 449–469.
Kortum, K., Machemehl, R.B., 2012. Free-Floating Carsharing Systems: Innovations in Membership Prediction, Mode Share, and Vehicle Allocation Optimization Methodologies. The University of Texas at Austin.
Lamotte, R., de Palma, A., Geroliminis, N., 2017. On the use of reservation-based autonomous vehicles for demand management. Transp. Res. Part B 99, 205–227.
Li, Q., Liao, F., Timmermans, H.J.P., Zhou, J., 2016. A user equilibrium model for combined activity-travel choice under prospect theoretical mechanisms of decision-making under uncertainty. Transportmetrica A 12, 629–649.
Li, Z.C., Lam, W.H.K., Wong, S.C., Sumalee, A., 2010. An activity-based approach for scheduling multimodal transit services. Transportation 37 (5), 751–774.
Liao, F., 2016. Modeling duration choice in space–time multi-state supernetworks for individual activity-travel scheduling. Transp. Res. Part C 69, 16–35.
Liao, F., Arentze, T.A., Timmermans, H.J.P., 2010. Supernetwork approach for multimodal and multi-activity travel planning. Transp. Res. Rec. 2175, 38–46.
Liao, F., Arentze, T.A., Timmermans, H.J.P., 2011. Constructing personalized transportation networks in multi-state supernetworks: a heuristic approach. Int. J. Geogr. Inf. Sci. 25 (11), 1885–1903.
Liao, F., Arentze, T.A., Timmermans, H.J.P., 2012. A supernetwork approach for modeling traveler response to park-and-ride. J. Transp. Res. Rec. 2323, 10–17.

Liao, F., Arentze, T.A., Timmermans, H.J.P., 2013a. Multi-state supernetwork framework for the two-person joint travel problem. Transportation 40 (4), 813–826.
Liao, F., Arentze, T.A., Timmermans, H.J.P., 2013b. Incorporating space–time constraints and activity-travel time profiles in a multi-state supernetwork approach to individual activity-travel scheduling. Transp. Res. Part B 55, 41–58.
Liao, F., Rasouli, S., Timmermans, H.J.P., 2014. Incorporating activity-travel time uncertainty and stochastic space–time prisms in multistate supernetworks for activity-travel scheduling. Int. J. Geogr. Inf. Sci. 28 (5), 928–945.
Liao, F., van Wee, B., 2016. Accessibility measures for robustness of the transport system. Transportation 44 (5), 1213–1233.
Liu, P., Liao, F., Huang, H.J., Timmermans, H.J.P., 2015. Dynamic activity-travel assignment in multi-state supernetworks. Transp. Res. Part B 81, 656–671.
Lo, H.K., Yip, C.W., Wan, K.H., 2003. Modeling transfer and nonlinear fare structure in multi-modal network. Transp. Res. Part B 37, 149–170.
Mahmassani, H.S., Liu, Y., 1999. Dynamics of commuting decision behaviour under advanced traveller information systems. Transp. Res. Part C 7, 91–107.
Morgen Stanley Report (*accessed on 11/15/2017*).
Mounce, R., Carey, M., 2011. Route swapping in dynamic traffic networks. Transp. Res. Part B 45 (1), 102–111.
Nagurney, A., 2004. Supernetworks: paradoxes, challenges and new opportunities. In: 1st 18 International Conference on the Economic and Social Implications of Information Technology, vol. 19, pp. 229–254.
Nagurney, A., Zhang, D., 1997. Projected dynamical systems in the formulation, stability analysis, and computation of fixed-demand traffic network equilibria. Transp. Sci. 31 (2), 147–158.
Nguyen, S., Dupuis, C., 1984. An efficient method for computing traffic equilibria in networks with asymmetric transportation costs. Transp. Sci. 18 (2), 185–202.
Nourinejad, M., Chow, J.Y., Roorda, M.J., 2016. Equilibrium scheduling of vehicle-to-grid technology using activity based modelling. Transp. Res. Part C 65, 79–96.
Nourinejad, M., Roorda, M.J., 2015. Carsharing operations policies: a comparison between one-way and two-way systems. Transportation 42 (3), 497–518.
Ramadurai, G., Ukkusuri, S., 2010. Dynamic user equilibrium model for combined activity-travel choices using activity-travel supernetwork representation. Netw. Spatial Econ. 10 (2), 273–292.
Schmöller, S., Weikl, S., Müller, J., Bogenberger, K., 2015. Empirical analysis of free-floating carsharing usage: the Munich and Berlin case. Transp. Res. Part C 56, 34–51.
Sheffi, Y., 1985. Urban Transportation Networks: Equilibrium Analysis with Mathematical Programming Methods. Prentice-Hall, Englewood Cliffs.
Simon, H., 1955. A behavioural model of rational choice. Q. J. Econ. 69, 99–118.
Szeto, W.Y., Lo, H.K., 2006. Dynamic traffic assignment: properties and extensions. Transportmetrica 2 (1), 31–52.
Weikl, S., Bogenberger, K., 2015. A practice-ready relocation model for free-floating carsharing systems with electric vehicles–mesoscopic approach and field trial results. Transp. Res. Part C 57, 206–223.
Whitehead, J., Haab, T., Huang, J.C., 2012. Preference Data For Environmental Valuation: Combining Revealed and Stated Approaches. Routledge, New York.
Ye, H., Yang, H., 2017. Rational behavior adjustment process with boundedly rational user equilibrium. Transportation Science doi.org/10.1287/trsc.2016.0715.
Zoepf, S.M., Keith, D.R., 2016. User decision-making and technology choices in the US carsharing market. Transp. Policy 51, 150–157.